

Performance of Dual-Hop Relaying for OWC System Over Foggy Channel with Pointing Errors and Atmospheric Turbulence

Ziyaur Rahman, *Graduate Student Member, IEEE*, Tejas Nimish Shah, S. M. Zafaruddin, *Senior Member, IEEE*, and V. K. Chaubey, *Senior Member, IEEE*

Abstract— Optical wireless communication (OWC) over atmospheric turbulence and pointing errors is a well-studied topic. Still, there is limited research on signal fading due to random fog and pointing errors in outdoor environments. In this paper, we analyze the performance of a decode-and-forward (DF) relaying under the combined effect of random fog, pointing errors, and atmospheric turbulence with a negligible line-of-sight (LOS) direct link. We consider a generalized model for the end-to-end channel with independent and not identically distributed (i.n.i.d.) pointing errors, random fog with Gamma distributed attenuation coefficient, asymptotic exponentiated Weibull turbulence, and asymmetrical distance between the source and destination. We derive distribution functions of the signal-to-noise ratio (SNR), and then we develop analytical expressions of the outage probability, average SNR, ergodic rate, and average bit error rate (BER) in terms of OWC system parameters. We also develop simplified performance to provide insight on the system behavior analytically under various practically relevant scenarios. We demonstrate the mutual effects of channel impairments and pointing errors on the OWC performance, and show that the relaying system provides significant performance improvement compared with the direct transmissions, especially when pointing errors and fog becomes more pronounced.

Index Terms—BER, exotic channels, fog, optical wireless communication, performance analysis, outage probability, pointing errors, relaying, SNR.

I. INTRODUCTION

Optical wireless communication (OWC) is a potential technology that transmits data through an unguided atmospheric channel in the unlicensed optical spectrum [1]–[3]. However, signal transmission at a small wavelength encounters different channel impairments such as atmospheric turbulence, pointing errors, and fog. The atmospheric turbulence is caused by the scintillation effect of light propagation whereas the pointing errors (i.e., misalignment between the transmitter and receiver) happens due to the dynamic wind loads, weak earthquakes, and thermal expansion [4], [5]. The impact of foggy conditions on OWC systems depends on the intensity of fog ranging between light, medium, and dense [6], [7]. Although turbulence and fog may not co-exist since both are inversely correlated with each other [4], [8], the effect of turbulence can not be ignored in

light foggy conditions. The combined effect of atmospheric turbulence, pointing errors, and fog has a detrimental effect on the signal quality and presents a major challenge in the OWC deployment in outdoor environments.

The use of relaying has been extensively studied to improve the performance of OWC systems under the effect of turbulence and/or pointing errors [9]–[24]. In the aforementioned and related research, the statistical effect of foggy channels combined with pointing errors and atmospheric turbulence has not been considered. Recent studies confirm that the signal attenuation in the fog is not deterministic but follows a probabilistic model [25]–[27]. In [26], the authors developed Johnson SB based probability distribution function (PDF) as a model for the random fog channel. They studied numerically the system performance in terms of average bit error rate (BER) and channel capacity. Considering the intractability of the Johnson SB for performance analysis, the authors in [27] proposed Gamma distribution for the signal attenuation in foggy weather and evaluated average signal-to-noise ratio (SNR), ergodic rate, outage probability, and BER. In our recent paper [28], we proposed a multi-aperture OWC system to mitigate the effect of fog. The authors in [29] presented ultrashort high-intensity laser filaments for high-bit-rate transmissions over the fog. These studies show that the OWC performance is significantly limited in dense fog but can provide acceptable performance in the light fog over shorter links. However, combining the effect of pointing errors with fog shows high degradation in performance even in light foggy conditions [30], [31]. The authors in [30] have considered three techniques to mitigate this effect: multi-hop relay systems using decode-and-forward (DF), active laser selection, and parallel radio frequency/free space optical (RF/FSO) link. Laser selection and hybrid transmission techniques require feedback from the receiver to the transmitter, thereby increasing the overhead. On the other hand, Multi-hop relaying requires channel state information (CSI) at each relay to decode the signal, which can be hard in practice. In [30], the outage probability of a multi-hop FSO system under the combined effect of fog and pointing errors has been analyzed. Analyzing the system performance using different performance metrics such as average SNR, ergodic rate, and average BER is desirable for an efficient deployment of OWC systems under the combined effect of fog and pointing errors. It is noted that there are no analyses of average SNR, ergodic rate, BER, and outage probability for the performance improvement of a relay-assisted OWC system under the statistical effect of random fog, pointing errors, and atmospheric turbulence.

In this paper, we analyze the end-to-end performance of a

This work was supported in part by the Start-up Research Grant, Science and Engineering Research Board (SERB), Department of Science and Technology (DST), India under Grant SRG/2019/002345.

Ziyaur Rahman (p20170416@pilani.bits-pilani.ac.in), Tejas Nimish Shah (t20170024@pilani.bits-pilani.ac.in), S. M. Zafaruddin (syed.zafaruddin@pilani.bits-pilani.ac.in), and V. K. Chaubey (vkc@pilani.bits-pilani.ac.in) are with the Department of Electrical and Electronics Engineering, Birla Institute of Technology and Science, Pilani, Pilani-333031, Rajasthan, India.

relay-assisted OWC system under the combined effect of fog, pointing errors, and atmospheric turbulence by considering a single DF relaying with no direct transmission to the destination. The major contributions of the paper are as follows:

- We consider a generalized model for the end-to-end channel of the relay-assisted system with independent and not identically distributed (i.n.i.d.) pointing errors, random fog with Gamma distributed attenuation coefficient, exponentiated Weibull turbulence, and asymmetrical distance between the source and destination. We assume independent and identically distributed (i.i.d.) atmospheric turbulence and random fog since these channel impairments may affect both links independently generated from the same probabilistic model.
- We derive a novel asymptotic PDF of the combined channel, and simplify the existing cumulative distribution function (CDF) of the channel with random fog and pointing errors in terms of a single incomplete gamma function and without involving the exponential integral.
- We derive analytical expressions of the outage probability, average SNR, ergodic rate, and average BER of the relay-assisted OWC system. The derived expressions are expressed in well-known mathematical functions and consist of a few summation terms over the shape parameter of the foggy channel. We show that the dual-hop relaying can mitigate fog, pointing errors, and turbulence-induced fading for high-speed OWC links.
- We show that there is a significant gap in the performance using the existing visibility range based path-loss computation as compared to the probabilistic modeling of fog and the effect of fading due to the atmospheric turbulence is negligible in the presence of fog.

A. Related Research

Traditionally, signal attenuation due to the fog was assumed to be deterministic and quantified using a visibility range, for example, less attenuation in light fog and more in the dense fog [6], [7], [26], [32]–[36]. Kruse model in [6] is based on experimental data, whereas Kim [7] used Mie scattering theory to predict the signal attenuation. The authors in [33] [34] updated the earlier models considering modified Gamma distribution for the particle size of fog. The authors in [35] developed a power delay model for the attenuation coefficient based on extensive measurement data. On the other hand, there are quite a few statistical models for the atmospheric turbulence, for example, log normal [37], Gamma-Gamma [38], Málaga [39], and \mathcal{F} -distribution [40]. Recently, Barrios and Dios [41] proposed the exponentiated Weibull (EW) distribution model for atmospheric turbulence. This model provides a good fit between simulation and experimental data under the moderate-to-strong turbulence for aperture averaging conditions, as well as for point-like apertures. A distinguishing feature of the EW model is its simple closed-form expression of the PDF [42]. It should be noted that the model of pointing errors [4] is used widely, assuming independent identical distributed Gaussian for the elevation and the horizontal displacement.

Relay-assisted communication is a potential technique to deal with the channel fading in wireless systems [43], [44]. Here, a single relay or many intermediate nodes can assist data transmission between a single source and destination. In particular, for OWC systems, there is a vast literature on the

relaying using amplify-and-forward (AF) and DF protocols in [9]–[15], all-optical relaying in [16]–[24], and relaying for hybrid RF/FSO systems in [45]–[52]. In the seminal work [9], multi-hop and cooperative relaying using AF and DF protocols have been considered for an aggregated channel model which takes into account both path-loss and turbulence-induced log-normal fading. The authors in [10] investigated a multi-hop relaying to mitigate the effect of fading in FSO systems over log-normal atmospheric turbulence channels. The end-to-end performance in terms of outage probability, the average BER, and the ergodic capacity for a multi-hop relaying with AF and DF protocols under the combined effect of Gamma-Gamma turbulence and pointing errors have been investigated in [11]. Although the complex multi-hop relaying can provide a better performance, a dual-hop relay system (with no direct link between the source and the destination) that selects a single relay opportunistically is considered in [12]. The authors in [13] studied the information-theoretic performance of parallel relaying for FSO communications over Gamma-Gamma fading channels with a single relay but with a line-of-sight link between the source and the destination. An optimal relay placement scheme for serial and parallel relaying along with a diversity gain analysis has been considered in [14]. The authors in [15] have considered the inter-relay cooperation on the outage probability and diversity order performance of the DF cooperative FSO communication systems.

An all-optical relaying scheme is efficient since signals are processed in the optical domain without requiring optical-to-electrical and electrical-to-optical conversions [16]–[24]. The references [21], [22] provided analytical expressions for the outage probability, average BER, and ergodic capacity over strong atmospheric turbulence channels with misalignment-induced pointing errors by considering a single optical AF relay with fixed and variable gain. Hybrid RF/FSO systems, where relays act as an interface between RF and optical links, have been studied [45]–[52]. A dual-hop relay system over the asymmetric links has been considered for both RF and FSO environments in [45] and derived exact expression for outage probability. The BER performance and the capacity analysis of an AF-based dual-hop mixed RF–FSO is presented in [46], where the RF links are Rayleigh distributed and FSO links are characterized by the Gamma–Gamma distributed turbulence and pointing errors. Considering a dual-hop transmission with a single-relay and ignoring the direct transmission, the authors in [48]–[50] have analyzed the OWC performance under the turbulence and pointing errors. The authors in [51] have considered an FSO/RF-FSO link adaptation scheme for hybrid FSO systems and analyzed different performance metrics like outage probability, average BER, and ergodic rate. Recently, a hybrid dual-hop relaying with mmWave and FSO scheme is studied in [52].

B. Notations and Organization

We list the main notations in Table I. This paper is organized as follows: In Section II, we discuss the relay assisted OWC system model. In Section III, we analyze the OWC system performance by deriving closed-form expressions for the outage probability, average SNR, ergodic rate, and average BER. In Section IV, the simulation results of the proposed system are presented. Finally, in Section V, we provide conclusions.

TABLE I
THE LIST OF MAIN NOTATIONS

$(\cdot)_1$	Notation for the first link
$(\cdot)_2$	Notation for the second link
y	Received signal
h	Random channel state
R	Detector responsivity
x	Transmit signal intensity
w	AWGN
P_t	Transmit power
d_1	Distance: transmitter to relay
d_2	Distance: relay and destination
d	$d_1 + d_2$
k	Shape parameter of foggy channel
β	Scale parameter of foggy channel
P_{out}	Outage probability
γ_0	SNR without fading
γ	SNR with fading
$\bar{\gamma}$	Average SNR
$\bar{\eta}$	Ergodic rate
P_e	Average BER
$\Gamma(a)$	$\int_0^\infty t^{a-1} e^{-t} dt$
$\Gamma(a, t)$	$\int_t^\infty s^{a-1} e^{-s} ds$
$Q(\gamma)$	$\frac{1}{\sqrt{2\pi}} \int_\gamma^\infty e^{-\frac{u^2}{2}} du$
$\text{erf}(\gamma)$	$\frac{2}{\sqrt{\pi}} \int_0^\gamma e^{-u^2} du$
${}_1F_1(a; b; z)$	$\sum_{k=0}^\infty \frac{\Gamma(a+k)\Gamma(b)}{\Gamma(a)\Gamma(b+k)} \frac{z^k}{k!}$

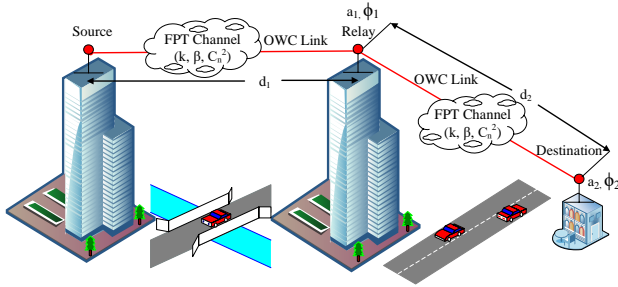


Fig. 1. Relay assisted OWC system.

II. SYSTEM MODEL

We consider an OWC system using intensity modulation/direct detection (IM/DD). It consists of a single-aperture transceiver system, with a negligible line-of-sight (LOS) direct link under fog, pointing errors, and atmospheric turbulence, as shown in Fig 1. The signal y at a receiver aperture is given as

$$y = h_f h_p h_t R x + w, \quad (1)$$

where x is the transmitted signal, R represents the detector responsivity (in amperes per watt), and w represents an additive white Gaussian noise (AWGN) with variance σ_w^2 . The terms h_f , h_p , and h_t are the random states of the foggy channel, pointing errors, and atmospheric turbulence induced fading, respectively.

We use the PDF of fog as given in [27]:

$$f_{h_f}(h_f) = \frac{z^k}{\Gamma(k)} \left(\ln \frac{1}{h_f} \right)^{k-1} h_f^{z-1}, \quad (2)$$

where $0 < h_f \leq 1$, $z = 4.343/\beta d$, $k > 0$ is the shape parameter and $\beta > 0$ is the scale parameter. It is noted that different pairs of k, β determine the severity of the foggy channel such as $\{k = 2.32, \beta = 13.12\}$, $\{k = 5.49, \beta = 12.06\}$, $\{k = 6.0, \beta = 23.06\}$ for light, moderate and thick foggy conditions, respectively. The PDF of pointing errors fading h_p is given in [4]:

$$f_{h_p}(h_p) = \frac{\rho^2}{A_0^2} h_p^{\rho^2-1}, 0 \leq h_p \leq A_0, \quad (3)$$

where $A_0 = \text{erf}(v)^2$ with $v = \sqrt{\pi/2} a/\omega_z$ and ω_z is the beam width, and $\rho = \frac{\omega_{z\text{eq}}}{2\sigma_s}$ with $\omega_{z\text{eq}}$ as the equivalent beam width at the receiver and σ_s as the variance of pointing errors displacement characterized by the horizontal sway and elevation [4]. Finally, the random atmospheric turbulence induced fading can be modeled over EW distribution with PDF [41]:

$$f_{h_t}(h_t) = \frac{\alpha_t \beta_t}{\eta_t} \left(\frac{h_t}{\eta_t} \right)^{\beta_t-1} \exp \left[- \left(\frac{h_t}{\eta_t} \right)^{\beta_t} \right] \times \left\{ 1 - \exp \left[- \left(\frac{h_t}{\eta_t} \right)^{\beta_t} \right] \right\}^{\alpha_t-1}, h_t \geq 0 \quad (4)$$

where $\beta_t > 0$ is the shape parameter of the scintillation index (SI), $\eta_t > 0$ is a scale parameter of the mean value of the irradiance and $\alpha_t > 0$ is an extra shape parameter that is strongly dependent on the receiver aperture size. The specific values of the parameters α, β and η as well as some expressions for evaluating these parameters is given in [41].

We denote by d_1 the distance between the source and relay and d_2 the distance between the relay and destination. For the case of relayed transmission using the DF protocol, the expressions for signals received at the relay and destination when x is the transmitted signal:

$$y_r = h_{f1} h_{p1} h_{t1} R_1 x + w_1 \quad (5)$$

$$y_d = h_{f2} h_{p2} h_{t2} R_2 x + w_2 \quad (6)$$

where h_{f1}, h_{p1}, h_{t1} and h_{f2}, h_{p2}, h_{t2} are random fog, pointing errors, and atmospheric turbulence channel states between source-relay and relay-destination, respectively, each having w_1 and w_2 as AWGNs. Note that $h_1 = h_{f1} h_{p1} h_{t1}$ is the combined channel between the source and the relay, and $h_2 = h_{f2} h_{p2} h_{t2}$ is the combined channel between the relay and destination.

We use a general relaying scenario $d_2 > d_1$ with different values of pointing errors parameters for both links giving an i.i.d fading model for pointing errors. However, we assume i.i.d. atmospheric turbulence and random fog since these channel impairments may affect both the links independently generated from the same probabilistic model. As a special case, we also consider that the relay is situated at the midway between the source and destination (i.e., $d_1 = d_2$) and that the channel parameters are same for both links (i.e., i.i.d. condition).

For comparison, we also consider a channel-assisted AF

such that the received signal at the destination is:

$$y_d = h_{f2}h_{p2}h_{t2}Gy_r + w_2 \quad (7)$$

where $G = \sqrt{\frac{P_t}{h_1^2 P_t^2 R_1^2 + \sigma_w^2}}$ is the relaying gain. The end-to-end SNR with the AF relaying is given by

$$\gamma = \frac{\gamma_1 \gamma_2}{\gamma_1 + \gamma_2 + 1} \quad (8)$$

It should be noted that the performance analysis using the AF relaying in closed form is intractable due to the underlying distribution function of the combined fog and pointing errors, as shown in Appendix D.

III. PERFORMANCE ANALYSIS

In this section, we analyze the performance of a relay-assisted system. First, we present an asymptotic expression for the PDF of SNR under the combined effect fog, pointing errors, and atmospheric turbulence, and an exact CDF expression under the combined effect fog, pointing errors. Next, we use the derived PDF's to analyze the outage probability, average SNR, ergodic rate, and average BER performance of the OWC system. The derived expressions show the system behavior in a relay-assisted environment under the combined effect of channel impairments that can help the network operator for an efficient design of relay-assisted OWC links.

A. Probability Distribution Functions

We define $\gamma = \gamma_0 |h|^2$ as the SNR, where $h = h_f h_p h_t$, $\gamma_0 = 2P_t^2 R^2 / \sigma_w^2$, and P_t is the average optical transmitted power. The probability distribution of the SNR γ is given in the following Proposition:

Proposition 1: The PDF of SNR γ under the combined effect of random fog, pointing errors, and atmospheric turbulence for the single OWC link is given as

$$f_\gamma(\gamma) = \frac{C^{(1)}}{\sqrt{\gamma\gamma_0}} \left(\sqrt{\frac{\gamma}{\gamma_0}} \right)^{\phi^2-1} - \frac{C^{(2)}}{\sqrt{\gamma\gamma_0}} \left(\sqrt{\frac{\gamma}{\gamma_0}} \right)^{\phi^2-1} \times \Gamma(k, m \ln(a/\sqrt{\gamma/\gamma_0})), \quad \gamma \leq a^2 \gamma_0 \quad (9)$$

where $f_\gamma(\gamma)$ is the exact PDF under the combined effect of the random fog and pointing errors with negligible turbulence with parameters $a = A_0$, $\phi = \rho$, and $f_\gamma(\gamma)$ is the asymptotic PDF for the combined channel effect of fog, pointing errors, and atmospheric turbulence with the parameters $a = \frac{\eta_t A_0}{(M_{r,2} \left(\frac{2\alpha_t \beta_t}{\omega_{z_{eq}}^2} \right)) \frac{1}{\alpha_t \beta_t}}$, $\phi = \sqrt{\alpha_t \beta_t}$, $C^{(1)} = \frac{z^k \phi^2}{2m^k a^{\phi^2}}$, and $C^{(2)} = \frac{C^{(1)}}{\Gamma(k)}$.

Proof: An exact PDF for the combined effect of pointing errors and fog (i.e., with $a = A_0$ and $\phi = \rho$ in (9)) is already derived in [30]. To include the effect of atmospheric turbulence, we use the asymptotic PDF of $h_{pt} = h_p h_t$ (i.e., combined effect of atmospheric turbulence and pointing errors) as given in [53]:

$$f_{h_{pt}}(h_{pt}) = \frac{\alpha_t \beta_t M_{r,2} \left(\frac{2\alpha_t \beta_t}{\omega_{z_{eq}}^2} \right)}{(\eta_t A_0)^{\alpha_t \beta_t}} h_{pt}^{\alpha_t \beta_t - 1}, \quad 0 \leq h_{pt} \leq a \quad (10)$$

where $a = \frac{\eta_t A_0}{(M_{r,2} \left(\frac{2\alpha_t \beta_t}{\omega_{z_{eq}}^2} \right)) \frac{1}{\alpha_t \beta_t}}$, and $M_{r,2}$ is the squared Beckmann distribution given as

$$M_{r,2}(t) = \frac{\exp\left(\frac{\mu_x^2 t}{1-2t\sigma_x^2} + \frac{\mu_y^2 t}{1-2t\sigma_y^2}\right)}{\sqrt{(1-2t\sigma_x^2)(1-2t\sigma_y^2)}} \quad (11)$$

Here, σ_x and σ_y represent different jitters for the horizontal displacement x and the elevation y , and μ_x and μ_y represent different boresight errors in each axis of the receiver plane, i.e. $x \sim N(\mu_x, \sigma_x)$ and $y \sim N(\mu_y, \sigma_y)$. The PDF of the combined channel $h = h_f h_{pt}$ can be expressed as [54]

$$f_h(h) = \int f_{h_{pt}|h_f}(h_{pt}|h_f) f_{h_f}(h_f) dh_f, \quad (12)$$

Using (2) and (10) in (12), we get

$$f_h(h) = \frac{\alpha_t \beta_t z^k h^{\alpha_t \beta_t - 1}}{a^{\alpha_t \beta_t} \Gamma(k)} \int_{h/a}^1 \left[\ln\left(\frac{1}{h_f}\right) \right]^{k-1} h_f^{m-1} dh_f \quad (13)$$

where $m = z - \alpha_t \beta_t$. Substituting $t = \ln(1/h_f)$ and using the identity [[7]-pp. 348], (13) yields

$$f_h(h) = \frac{\alpha_t \beta_t z^k}{a^{\alpha_t \beta_t} \Gamma(k) m^k} h^{\alpha_t \beta_t - 1} [\Gamma(k) - \Gamma(k, m \ln(a/h))] \quad (14)$$

Substituting $\phi = \sqrt{\alpha_t \beta_t}$ and $h = \sqrt{\frac{\gamma}{\gamma_0}}$ in (14), we get the asymptotic PDF of SNR for the combined effect of fog, pointing errors, and atmospheric turbulence in (9). ■

It is interesting to note that the form of PDF is similar in both cases facilitating a unified performance analysis with and without atmospheric turbulence. Further, we show in Section IV using numerical analysis that the asymptotic performance with atmospheric turbulence is close to the exact results.

Proposition 2: The CDF of the SNR for a single link under foggy channel with pointing errors and atmospheric turbulence is given as

$$F_\gamma(\gamma) = D^{(1)} \left(\frac{a}{\sqrt{\gamma/\gamma_0}} \right)^{-\phi^2} - D^{(2)} (k-1)! \times \sum_{i=0}^{k-1} \frac{m^i z^{-i-1}}{i!} \Gamma(i+1, z \ln(a/\sqrt{\gamma/\gamma_0})) \quad (15)$$

where $D^{(1)} = \frac{z^k}{m^k}$ and $D^{(2)} = \frac{D^{(1)} \phi^2}{\Gamma(k)}$ are constants.

Proof: Substituting $u = \ln\left(\frac{a}{\sqrt{\gamma/\gamma_0}}\right)$ in the second term of (9), the CDF $F_\gamma(\gamma) = \int_0^\gamma f(\gamma) d\gamma$ is given as:

$$F_\gamma(\gamma) = D^{(1)} \left(\frac{a}{\sqrt{\gamma/\gamma_0}} \right)^{-\phi^2} - D^{(2)} \int_u^\infty e^{-\phi^2 u} \Gamma[k, mu] du \quad (16)$$

Using $\Gamma(a, t) \triangleq (a-1)! e^{-t} \sum_{m=0}^{a-1} \frac{t^m}{m!}$ in (16), and applying the definition of incomplete Gamma function, we get (15). ■

It should be noted that the derived CDF in (15) is different from the CDF of [30]: it consists of a single incomplete gamma function without the exponential integral, and can be useful for performance analysis in a closed-form using integer k .

Now, we discuss the distribution functions with DF relaying. We assume equal transmit power at the source and relay (i.e., $P_t = P_r$) to get the instantaneous SNRs of signals received at the relay and receiver as $\gamma_1 = \gamma_0 h_1^2$ and $\gamma_2 = \gamma_0 h_2^2$,

respectively. Assuming that γ_1 and γ_2 are independent for analytical tractability, the expression of end-to-end SNR for the DF relaying is given as:

$$\gamma = \min(\gamma_1, \gamma_2) \quad (17)$$

It is true that k and β parameters of the random foggy channel will be identical in both the hops. However, channel realizations at two distinct points separated over several hundred meters might not be the same. The i.i.d. assumption on the foggy channel has been considered in [30].

The CDF and PDF of end-to-end SNR for DF relaying scheme can be given as [21]:

$$F(\gamma) = F_1(\gamma) + F_2(\gamma) - F_1(\gamma)F_2(\gamma) \quad (18)$$

$$f(\gamma) = f_1(\gamma) + f_2(\gamma) - f_1(\gamma)F_2(\gamma) - f_2(\gamma)F_1(\gamma) \quad (19)$$

where $f_1(\gamma)$, $f_2(\gamma)$ are the PDF of the first link and second link, respectively. Similarly, $F_1(\gamma)$ and $F_2(\gamma)$ are the CDF of the first link and the second link, respectively.

It is seen that distribution functions in (9) and (15) involves incomplete gamma functions with logarithmic argument requiring novel approaches to performance analysis. The use of simple approximation of incomplete Gamma function $\Gamma[k, m \ln u] \approx u^{-m} (m \ln u)^{k-1}$ can simplify the analysis, but the derived approximate expressions grossly overestimate/underestimate the exact performance.

B. Outage Probability

Outage probability is a performance measure to demonstrate the effect of the fading channel. It is defined as the probability of failing to reach an SNR threshold value γ_{th} , i.e., $P_{out} = P(\gamma < \gamma_{th})$.

Proposition 3: If k and β are the parameters of foggy channel, a_1 , a_2 and ϕ_1 , ϕ_2 are the channel parameters (of pointing errors and atmospheric turbulence), then an exact closed-form expression for the outage probability is given as

$$P_{out} = P_{out_1} + P_{out_2} - P_{out_1}P_{out_2}, \quad (20)$$

where outage probabilities of source-to-relay (P_{out_1}) and relay-to-source (P_{out_2}) are

$$P_{out_1} = D_1^{(1)} \left(\frac{a_1^2 \gamma_0}{\gamma_{th}} \right)^{-\frac{\phi_1^2}{2}} - D_1^{(2)} (k-1)! \left(\frac{a_1^2 \gamma_0}{\gamma_{th}} \right)^{-\frac{z_1}{2}} \sum_{i=0}^{k-1} \sum_{j=0}^i \frac{m_1^i z_1^{j-i-1} \left(\ln \left(\frac{a_1 \sqrt{\gamma_0}}{\sqrt{\gamma_{th}}} \right) \right)^j}{j!} \quad (21)$$

$$P_{out_2} = D_2^{(1)} \left(\frac{a_2^2 \gamma_0}{\gamma_{th}} \right)^{-\frac{\phi_2^2}{2}} - D_2^{(2)} (k-1)! \left(\frac{a_2^2 \gamma_0}{\gamma_{th}} \right)^{-\frac{z_2}{2}} \sum_{i=0}^{k-1} \sum_{j=0}^i \frac{m_2^i z_2^{j-i-1} \left(\ln \left(\frac{a_2 \sqrt{\gamma_0}}{\sqrt{\gamma_{th}}} \right) \right)^j}{j!} \quad (22)$$

where $z_1 = 4.343/\beta d_1$, $z_2 = 4.343/\beta d_2$ with $d_2 \geq d_1$ as the transmission link lengths for a relay-assisted OWC system.

Proof: Using $\gamma = \gamma_{th}$, $m_1 = z_1 - \phi_1^2$, $m_2 = z_2 - \phi_2^2$ and series expansion of incomplete Gamma function $\Gamma(a, t) \triangleq (a-1)! e^{-t} \sum_{m=0}^{a-1} \frac{t^m}{m!}$ [55] in (15), we get the term in (21) and (22), thus (20). ■

It is well known that the diversity order of the FSO channel with atmospheric turbulence (Gamma-Gamma model with parameters $\alpha_{\text{gamma}}, \beta_{\text{gamma}}$) and pointing errors is given as

$M = \frac{1}{2} \min\{\alpha_{\text{gamma}}^2, \beta_{\text{gamma}}^2, \phi^2\}$ [56], [57]. Using (20) and following the similar steps of [31], the diversity order can be derived as $M = \frac{1}{2} \min\{\phi_1^2, \phi_2^2, z_1, z_2\}$. The expression shows various possibilities of mitigating the impact of pointing errors and fog. For example, under certain conditions $M = \frac{z_1}{2} = \frac{2.171}{\beta d_1}$, and thus the performance depends only on the fog parameter β and source-to-relay distance d_1 .

C. Average SNR and Ergodic Rate

The average SNR and ergodic rate performance is computed using the PDF of SNR, which is given in (19). Thus, expressions for the average SNR and ergodic rate for IM/DD [10]:

$$\bar{\gamma} = \int_0^{\min(a_1^2 \gamma_0, a_2^2 \gamma_0)} \gamma f(\gamma) d\gamma \quad (23)$$

$$\bar{\eta} = \int_0^{\min(a_1^2 \gamma_0, a_2^2 \gamma_0)} \log_2(1 + \frac{e}{2\pi} \gamma) f(\gamma) d\gamma \quad (24)$$

It is noted that we have assumed that relay requires negligible time to relay the data while computing the ergodic rate. Further, considering the shorter symbol duration (in the range of few nanoseconds), the OWC channel can be considered a slow-fading channel [27]. We analyze the ergodic rate performance to provide an estimate on the throughput of the system. It should be noted that there is a vast literature on the ergodic rate performance on the slow fading FSO channels (See [11], [21], [22], and references therein).

Theorem 1: If k and β are the parameters of the foggy channel, a_1 , a_2 , ϕ_1 , and ϕ_2 are the channel parameters (of pointing errors and atmospheric turbulence), and $z_1 = 4.343/\beta d_1$, $z_2 = 4.343/\beta d_2$ with $d_2 \geq d_1$, then a closed-form expression of average SNR and a lower bound on ergodic rate are given by

$$\bar{\gamma} = \mathcal{F}_\gamma(a_1, a_2, \phi_1, \phi_2, z_1, z_2, k)$$

$$\bar{\eta} = \mathcal{F}_\eta(a_1, a_2, \phi_1, \phi_2, z_1, z_2, k)$$

where $\mathcal{F}_\gamma(a_1, a_2, \phi_1, \phi_2, z_1, z_2, k)$ and $\mathcal{F}_\eta(a_1, a_2, \phi_1, \phi_2, z_1, z_2, k)$ are given in (45) and (46) (in Appendix A), respectively.

Proof: We use the upper limit of the integration as $a_2^2 \gamma_0$ since $d_2 \geq d_1 \rightarrow a_2 \leq a_1$. We substitute (9) and (15) in (19) to get $f(\gamma)$ in terms of system parameters. Since each $f_1(\gamma)$, $f_2(\gamma)$, $F_1(\gamma)$, and $F_2(\gamma)$ consist of two terms resulting into twelve terms of integration in (23). We use $m_1 = (z_1 - \phi_1^2)$, $m_2 = (z_2 - \phi_2^2)$ and the series expansion $\Gamma(a, t) \triangleq (a-1)! e^{-t} \sum_{m=0}^{a-1} \frac{t^m}{m!}$, and substitute $u = \frac{a_1}{\sqrt{\gamma/\gamma_0}}$, and $v = \frac{a_2}{\sqrt{\gamma/\gamma_0}}$ to simplify the integrations into algebraic functions. Apart from simple integrations, we also encounter the following integration terms:

$$\int_1^\infty u^{-n} (\ln(u))^p du, \int_a^\infty u^{-n-3} (\ln(u))^p du, \int_1^\infty u^{-n} \Gamma[k, n \ln u] du \quad (25)$$

We solve the integrations of (25) in closed-forms, as represented in Appendix B. Using (47), (48) and (49) of Appendix B in (23) with some algebraic simplifications, we get (45) of Theorem 1. Similarly, to obtain the ergodic rate, we use the

inequality $\log_2(1 + \gamma) \geq \log_2(\gamma)$ in (24) and follow the same procedure used in deriving the average SNR expression. Here, in addition to terms in (25), we also need to integrate the following:

$$\int_1^{\infty} u^{-n} (\ln(au))^p (\ln(u))^t du \quad (26)$$

A closed-form expression of (26) is given in Appendix B. Thus, using (47), (48), (49), and (51) of Appendix B in (24), we get (46) of Theorem 1. ■

In the following Lemma 1, we simplify the derived expression by considering an i.i.d model and when the relay is located in the middle of the source and the destination.

Lemma 1: If k and β are the parameters of the foggy channel, a and ϕ are the parameters of pointing errors, and a relay is at the mid-point with $z = 8.686/\beta d$, then a closed-form expression of average SNR and a lower bound on the ergodic rate are:

$$\bar{\gamma} = \mathcal{F}_{\gamma}(a, \phi, z, k) \quad (27)$$

$$\bar{\eta} = \mathcal{F}_{\eta}(a, \phi, z, k) \quad (28)$$

where $\mathcal{F}_{\gamma}(a, \phi, z, k)$ and $\mathcal{F}_{\eta}(a, \phi, z, k)$ are given in (31) and (32) respectively.

Proof: Using (19) in (23) and (24), and noting that $a_1 = a_2 = a$, and $\phi_1 = \phi_2 = \phi$ under the symmetric i.i.d fading model, we get:

$$\bar{\gamma} = 2 \int_0^{a^2 \gamma_0} \gamma [f_{\gamma}(\gamma) - f_{\gamma}(\gamma)F_{\gamma}(\gamma)] d\gamma \quad (29)$$

$$\bar{\eta} = 2 \int_0^{a^2 \gamma_0} \log_2(1 + \frac{e}{2\pi} \gamma) [f_{\gamma}(\gamma) - f_{\gamma}(\gamma)F_{\gamma}(\gamma)] d\gamma \quad (30)$$

Substituting $u = \frac{a}{\sqrt{\gamma/\gamma_0}}$, $m = (z_r - \phi^2)$ and using series expansion $\Gamma(a, t) \triangleq (a-1)! e^{-t} \sum_{m=0}^{a-1} \frac{t^m}{m!}$ in (29) for the average SNR and (30) with the inequality $\log_2(1 + \gamma) \geq \log_2(\gamma)$ for the ergodic rate, we encounter some simple integration terms along with the first and third integration terms of (25). Using (47) and (49) of Appendix B with some algebraic simplifications, we get (27) and (28) of Lemma 1. ■

Further, we consider light foggy conditions (i.e., $k = 2$) to derive simple analytical expressions on the average SNR and ergodic rate for the i.i.d model in the following Corollary.

Corollary 1: If $k = 2$ and β are the parameters of the foggy channel, a and ϕ are the parameters of pointing errors, and relay is at the mid-point with $z = 8.686/\beta d$, then a closed-form expression of average SNR and a lower bound on the ergodic rate are given as

$$\bar{\gamma} = 2(a\phi z)^2 \gamma_0 \left(\frac{1}{(2+\phi^2)(2+z)^2} - \frac{2(1+z)^3 + \phi^4(1+2z) + \phi^2(3+4z(2+z))}{4(1+\phi^2)(1+z)^3(2+\phi^2+z)^2} \right) \quad (33)$$

$$\begin{aligned} \bar{\eta} \geq & \log_2\left(\frac{e}{2\pi}\right) + 2 \left(\left(\frac{\phi^2 z (2 \ln a + \ln \gamma_0) - 2(2\phi^2 + z)}{\phi^2 z \ln 2} \right) \right. \\ & - 0.36(\phi^2(\phi^2 + z)^{-2} - 2\phi^{-2} - 5z^{-1} - \\ & \left. 3(\phi^2 + z)^{-1} + 4 \ln a + 2 \ln \gamma_0) \right) \quad (34) \end{aligned}$$

Proof: The proof follows the similar procedure used in Lemma 1 with $k = 2$. ■

In our earlier work [31], we have shown that the average SNR without relaying is $\bar{\gamma}_{\text{direct}} = \frac{(za\phi)^2 \gamma_0}{(2+\phi^2)(2+z_{\text{direct}})^2}$, where $z_{\text{direct}} = 4.343/\beta d$. Thus, the first term in (33) corresponds to twice of the average SNR without relaying. Since the negative term in (33) is insignificant, we expect a higher average SNR with relaying. Similar conclusions can be made for the ergodic rate performance. These have been extensively studied through numerical analysis in Section IV.

Finally, we demonstrate the impact of randomness in the path loss due to the fog by considering that the fog causes a deterministic path gain $L = e^{-\psi d}$, where d is the link distance (in km) and ψ is the atmospheric attenuation factor, which depends on the visibility range and may depend on the wavelength [7].

Corollary 2: If the fog causes a deterministic path loss $L_r = e^{-\psi d/2}$ with relay-assisted transmission $d_1 = d_2 = d/2$ for an i.i.d fading model under random pointing errors and atmospheric turbulence, then asymptotic expressions of average SNR and ergodic rate are given as

$$\begin{aligned} \bar{\gamma} &= \frac{(aL_r)^2 \phi^4 \gamma_0}{(2+3\phi^2+\phi^4)}, \\ \bar{\eta} &= \log_2\left(\frac{e}{2\pi}\right) + \frac{1.4427(\phi^2 \ln((aL_r)^2 \gamma_0) - 3)}{\phi^2} \quad (35) \end{aligned}$$

Proof: Substituting $h_{pt} = \sqrt{\frac{\gamma}{\gamma_0}}$ in (10), we get an asymptotic PDF of the SNR for an OWC system under the combined effect of atmospheric turbulence and pointing errors with atmospheric path gain:

$$f_{\gamma}(\gamma) = \frac{\phi^2}{2\sqrt{\gamma\gamma_0}(aL)^{\phi^2}} \left(\sqrt{\frac{\gamma}{\gamma_0}} \right)^{\phi^2-1}, 0 \leq \gamma \leq (aL)^2 \gamma_0 \quad (36)$$

Using (36) and the CDF $F_{\gamma}(\gamma) = \int_0^{\gamma} f(\gamma) d\gamma$ in (29) and (30), it is straightforward to prove (35). ■

Comparing (31) and (32) with the expressions in (35) shows that the randomness in fog significantly complicates the system analysis. Further, the attenuation coefficient using deterministic path loss may overestimate/underestimate the performance obtained with the random fog distribution.

To compare with the relayed transmissions, we also find the average SNR and ergodic for the direct link d with $L = e^{-\psi d}$:

$$\begin{aligned} \bar{\gamma} &= \frac{\phi^2 (aL)^2}{2+\phi^2} \gamma_0, \\ \bar{\eta} &= \log_2\left(\frac{e}{2\pi}\right) + \frac{2}{\log(4)\phi^2} \left(-2 + \phi^2 \log((aL)^2 \gamma_0) \right) \quad (37) \end{aligned}$$

D. Average BER

In this subsection, we derive the average BER for the proposed relay-assisted scheme. Assuming IM/DD with on-off keying (OOK) modulation, the BER can be obtained as [58]:

$$P_e(\gamma) = AQ(\sqrt{B\gamma}) \quad (39)$$

$$\begin{aligned} \mathcal{F}_\gamma(a, \phi, z, k) &= 2 \left(\frac{2C^{(1)} a^{2+\phi^2} \gamma_0}{(2+\phi^2)} + 2C^{(2)} a^{2+\phi^2} \gamma_0 \frac{\left(-1 + \left(\frac{z-\phi^2}{2+z}\right)^k\right) \Gamma[k]}{(2+\phi^2)} - \frac{C^{(1)} D^{(1)} a^{2+\phi^2} \gamma_0}{(1+\phi^2)} + C^{(1)} D^{(2)} (k-1)! \right. \\ &\times \sum_{i=0}^{k-1} \frac{m^i z^{-i-1}}{i!} \frac{\Gamma(i+1) (\phi^2+z+2)^{-i-1} \left((\phi^2+z+2)^{i+1} - z^{i+1}\right)}{\phi^{2+2}} - C^{(2)} D^{(1)} a^{2+\phi^2} \gamma_0 \frac{\left(-1 + \left(\frac{m}{2+m+2\phi^2}\right)^k\right) \Gamma[k]}{(1+\phi^2)} \\ &\left. - C^{(2)} D^{(2)} a^{\phi^2+2} i! ((k-1)!)^2 \sum_{i=0}^{k-1} \sum_{j=0}^{k-1} \sum_{t=0}^i \frac{m^{i+j} z^{t-i-1} \Gamma(j+t+1)}{i! j! t! (\phi^2+2)^{j+t+1}} \right) \end{aligned} \quad (31)$$

$$\begin{aligned} \mathcal{F}_\eta(a, \phi, z, k) &= \log_2\left(\frac{e}{2\pi}\right) + 2.8854 \left(\frac{2C^{(1)} a^{\phi^2} (-2+\phi^2 \ln(a^2 \gamma_0))}{\phi^4} - 2C^{(2)} a^{\phi^2} (k-1)! \sum_{i=0}^{k-1} \frac{m^i (-2(1+i)+z \ln(a^2 \gamma_0))}{z^{2+i}} - \right. \\ &\frac{C^{(1)} D^{(1)} a^{\phi^2} (-1+\phi^2 \ln(a^2 \gamma_0))}{\phi^4} + 2C^{(1)} D^{(2)} a^{\phi^2} (k-1)! \sum_{i=0}^{k-1} \sum_{j=0}^i \frac{m^i z^{j-i-1} (-2(1+j)+(\phi^2+z) \ln(a^2 \gamma_0))}{(\phi^2+z)^{2+j}} + \\ &2C^{(2)} D^{(1)} a^{\phi^2} (k-1)! \sum_{i=0}^{k-1} \frac{m^i (-2(1+i)+(\phi^2+z) \ln(a^2 \gamma_0))}{(\phi^2+z)^{2+i}} + \\ &\left. C^{(2)} D^{(2)} a^{\phi^2} ((k-1)!)^2 \sum_{i=0}^{k-1} \sum_{j=0}^{k-1} \sum_{t=0}^i \frac{m^{i+j} z^{-i-j-3} (j+t)! (1+j+t-z \ln(a^2 \gamma_0))}{j! t! 2^{j+t}} \right) \end{aligned} \quad (32)$$

where $A = 1$ and $B = \frac{1}{2}$ for OOK modulation. However, we use the CDF in (18) to derive the average BER \bar{P}_e as [59]

$$\begin{aligned} \bar{P}_e &= - \int_0^{\min(a_1^2 \gamma_0, a_2^2 \gamma_0)} \frac{dP_e(\gamma)}{d\gamma} F(\gamma) d\gamma \\ &= A \sqrt{\frac{B}{8\pi}} \int_0^{\min(a_1^2 \gamma_0, a_2^2 \gamma_0)} \gamma^{-\frac{1}{2}} e^{-\frac{B\gamma}{2}} F(\gamma) d\gamma \end{aligned} \quad (40)$$

A general solution to the integration in (40) is intractable due to the exponential function and incomplete Gamma function with logarithmic argument raised to the power k . A general expression is intractable even with the application of Meijer's G representation.

We derive a closed-form expression for the average BER for a particular integer value of k (i.e., $k = 2$, $k = 3$, and so on). Specifically, we consider light foggy condition (with a shape parameter $k = 2$) and general pointing errors with asymptotic atmospheric turbulence to provide exact closed-form expression on the average BER. As noted in [30], the OWC performance is not sufficient for high-speed data transmission under moderate ($k > 2$) foggy conditions with pointing errors. It is also noted that light foggy conditions represent many OWC scenarios [34], [60].

Theorem 2: If $k = 2$ and β are the parameters of the foggy channel, a_1 , a_2 and ϕ_1 , ϕ_2 are the parameters of pointing errors and atmospheric turbulence, and $z_1 = 4.343/\beta d_1$, $z_2 = 4.343/\beta d_2$ with $d_2 \geq d_1$, then closed-form expression of average BER is:

$$\bar{P}_e = \mathcal{F}_{P_e}(a_1, a_2, \phi_1, \phi_2, z_1, z_2) \quad (41)$$

where $\mathcal{F}_{P_e}(a_1, a_2, \phi_1, \phi_2, z_1, z_2)$ is given in (38).

Proof: First, we substitute (18) and (15) in (40). We use $m_1 = (z_1 - \phi_1^2)$, $m_2 = (z_2 - \phi_2^2)$ and the series expansion $\Gamma(a, t) \triangleq (a-1)! e^{-t} \sum_{m=0}^{a-1} \frac{t^m}{m!}$, and substitute $u = \frac{a_1}{\sqrt{\gamma/\gamma_0}}$, and $v = \frac{a_2}{\sqrt{\gamma/\gamma_0}}$ to simplify the integrations into algebraic functions. Apart from simple integration terms, we

also encounter the following terms:

$$\begin{aligned} \int_1^\infty u^{-n-2} e^{-\frac{v}{u^2}} du, \int_a^\infty u^{-n-2} e^{-\frac{v}{u^2}} \ln(u) du, \\ \int_1^\infty u^{-n-2} e^{-\frac{v}{u^2}} \ln^2(u) du \end{aligned} \quad (42)$$

We provide closed-form expressions of (42) in Appendix C. Using (52), (53), and (54) of Appendix C with some algebraic simplifications, we get the (41) of Theorem 2. ■

Similarly, the average BER expression for other values of k can be obtained. It should be noted that the use of PDF to derive the average BER results into more terms compared to the CDF based approach of (40). Although the average BER in (38) consists of many terms, it is useful in analyzing the system performance using known mathematical functions in contrast to a single-term integral representation in (40). To simplify the underlying expressions, we consider deterministic path loss in the following Corollary.

Corollary 3: If the fog causes a deterministic path loss $L_r = e^{-\psi d/2}$ with relay-assisted transmission $d_1 = d_2 = d/2$ for an i.i.d fading model under random pointing errors and atmospheric turbulence, then an asymptotic expression of average BER is given as

$$\begin{aligned} \bar{P}_e &= \frac{2^{-1+\frac{\phi^2}{2}} A \sqrt{\pi}}{((aL)^2 B \gamma_0)^{\frac{\phi^2}{2}}} \left[2^{\frac{\phi^2}{2}} \left(\Gamma\left(\frac{1}{2} + \phi^2, \frac{(aL)^2 B \gamma_0}{2}\right) - \Gamma\left(\frac{1}{2} + \phi^2\right) \right) \right. \\ &\left. + 2((aL)^2 B \gamma_0)^{\frac{\phi^2}{2}} \left(\Gamma\left(\frac{1+\phi^2}{2}\right) - \Gamma\left(\frac{1+\phi^2}{2}, \frac{(aL)^2 B \gamma_0}{2}\right) \right) \right] \end{aligned} \quad (43)$$

Proof: Using (18) in (40), and noting that $a_1 = a_2 = a$, and $\phi_1 = \phi_2 = \phi$ under the symmetric i.i.d fading model, we get:

$$\bar{P}_e = A \sqrt{\frac{B}{8\pi}} \int_0^{\min(a_1^2 \gamma_0, a_2^2 \gamma_0)} \gamma^{-\frac{1}{2}} e^{-\frac{B\gamma}{2}} [2F_\gamma(\gamma) - (F_\gamma(\gamma))^2] d\gamma \quad (44)$$

Using (36) and substituting $F_\gamma(\gamma) = \int_0^\gamma f(\gamma) d\gamma$ in (44) and applying the definition of Gamma function and incomplete Gamma function, we get (43). ■

Similar to the average SNR and ergodic capacity, it can be seen from (43) that the consideration of deterministic path loss simplifies the BER expression compared with the random path

$$\begin{aligned}
\mathcal{F}_{P_e}(a_1, a_2, \phi_1, \phi_2, z_1, z_2) &= \frac{AD_1^{(1)}P_1^{-\frac{\phi_1^2}{2}}}{2\sqrt{\pi}} \left(\Gamma\left(\frac{1}{2}(1+\phi_1^2)\right) - \Gamma\left(\frac{1}{2}(1+\phi_1^2), P_2\right) \right) - \frac{AD_1^{(2)}P_1^{-\frac{z_1}{2}}}{2\sqrt{\pi z_1}} \\
&\times \left[\left(\Gamma\left(\frac{1}{2}(1+z_1)\right) - \Gamma\left(\frac{1}{2}(1+z_1), P_2\right) \right) \left(1 + \frac{m_1}{z_1}\right) + \frac{m_1}{2} \left(\Gamma\left(\frac{1}{2}(1+z_1), \frac{a_2^2 P_1}{a_1^2}\right) \ln \frac{a_2^2}{a_1^2} + \right. \right. \\
&\left. \left. G_{3,0}^{2,3} \left(0, 0, \frac{1}{2}(1+z_1) \middle| \frac{a_2^2 P_1}{a_1^2}\right) + \Gamma\left(\frac{1}{2}(1+z_1)\right) (\ln P_1 - \psi^{(0)}\left(\frac{1+z_1}{2}\right)) \right) \right] + \frac{AD_2^{(1)}P_2^{-\frac{\phi_2^2}{2}}}{2\sqrt{\pi}} \\
&\times \left(\Gamma\left(\frac{1}{2}(1+\phi_2^2)\right) - \Gamma\left(\frac{1}{2}(1+\phi_2^2), P_2\right) \right) - \frac{AD_2^{(2)}P_2^{-\frac{z_2}{2}}}{2\sqrt{\pi z_2}} \left[\left(\Gamma\left(\frac{1}{2}(1+z_2)\right) - \Gamma\left(\frac{1}{2}(1+z_2), P_2\right) \right) \left(1 + \frac{m_2}{z_2}\right) \right. \\
&\left. + \frac{m_2}{2} \left(G_{3,0}^{2,3} \left(0, 0, \frac{1}{2}(1+z_2) \middle| P_2\right) + \Gamma\left(\frac{1}{2}(1+z_2)\right) (\ln P_2 - \psi^{(0)}\left(\frac{1+z_2}{2}\right)) \right) \right] - \\
&\frac{AD_1^{(1)}D_2^{(1)}P_1^{-\frac{\phi_1^2}{2}}P_2^{-\frac{\phi_2^2}{2}}}{2\sqrt{\pi}} \left(\Gamma\left(\frac{1}{2}(1+\phi_1^2+\phi_2^2)\right) - \Gamma\left(\frac{1}{2}(1+\phi_1^2+\phi_2^2), P_2\right) \right) + \\
&\frac{AD_1^{(1)}D_2^{(2)}}{2\sqrt{\pi z_2}} \left[P_1^{-\frac{\phi_1^2}{2}}P_2^{-\frac{z_2}{2}} \left(\Gamma\left(\frac{1}{2}(1+\phi_1^2+z_2)\right) - \Gamma\left(\frac{1}{2}(1+\phi_1^2+z_2), P_2\right) \right) \left(1 + \frac{m_2}{z_2}\right) + \right. \\
&\left. \frac{m_2 P_2^{\frac{1}{2}(-\phi_1^2-z_2)}}{2\left(\frac{a_1}{a_2}\right)^{\phi_1^2}} \left(G_{3,0}^{2,3} \left(0, 0, \frac{1}{2}(1+\phi_1^2+z_2) \middle| P_2\right) + \Gamma\left(\frac{1}{2}(1+\phi_1^2+z_2)\right) (\ln P_2 - \psi^{(0)}\left(\frac{1+\phi_1^2+z_2}{2}\right)) \right) \right] \\
&+ \frac{AD_1^{(2)}D_2^{(1)}}{2\sqrt{\pi z_1}} \left[P_1^{-\frac{z_1}{2}}P_2^{-\frac{\phi_2^2}{2}} \left(\Gamma\left(\frac{1}{2}(1+\phi_2^2+z_1)\right) - \Gamma\left(\frac{1}{2}(1+\phi_2^2+z_1), P_2\right) \right) \left(1 + \frac{m_1}{z_1}\right) + \right. \\
&\left. \frac{m_1 P_1^{\frac{1}{2}(-\phi_2^2-z_1)}}{2\left(\frac{a_2}{a_1}\right)^{\phi_2^2}} \left(\Gamma\left(\frac{1}{2}(1+\phi_2^2+z_1), \frac{a_2^2 P_1}{a_1^2}\right) \ln \frac{a_2^2}{a_1^2} + G_{3,0}^{2,3} \left(0, 0, \frac{1}{2}(1+\phi_2^2+z_1) \middle| \frac{a_2^2 P_1}{a_1^2}\right) + \right. \\
&\left. \left. \Gamma\left(\frac{1}{2}(1+\phi_2^2+z_1)\right) (\ln P_1 - \psi^{(0)}\left(\frac{1+\phi_2^2+z_1}{2}\right)) \right) \right] - \\
&\frac{AD_1^{(2)}D_2^{(2)}}{2\sqrt{\pi z_1 z_2}} \left[P_1^{-\frac{z_1}{2}}P_2^{-\frac{z_2}{2}} \left(\Gamma\left(\frac{1}{2}(1+z_1+z_2)\right) - \Gamma\left(\frac{1}{2}(1+z_1+z_2), P_2\right) \right) \left(1 + \frac{m_1}{z_1} + \frac{m_2}{z_2} + \frac{m_1 m_2}{z_1 z_2}\right) + \right. \\
&\left. \frac{m_2 P_2^{\frac{1}{2}(-z_1-z_2)}}{2\left(\frac{a_1}{a_2}\right)^{z_1}} \left(G_{3,0}^{2,3} \left(0, 0, \frac{1}{2}(1+z_1+z_2) \middle| P_2\right) + \Gamma\left(\frac{1}{2}(1+z_1+z_2)\right) (\ln P_2 - \psi^{(0)}\left(\frac{1+z_1+z_2}{2}\right)) \right) \left(1 + \frac{m_1}{z_1}\right) \right) \\
&+ \frac{m_1 P_1^{\frac{1}{2}(-z_1-z_2)}}{2\left(\frac{a_2}{a_1}\right)^{z_2}} \left(\Gamma\left(\frac{1}{2}(1+z_1+z_2), \frac{a_2 P_1}{a_1}\right) \ln \frac{a_2}{a_1} + G_{3,0}^{2,3} \left(0, 0, \frac{1}{2}(1+z_1+z_2) \middle| \frac{a_2^2 P_1}{a_1^2}\right) + \right. \\
&\left. \Gamma\left(\frac{1}{2}(1+z_1+z_2)\right) (\ln P_1 - \psi^{(0)}\left(\frac{1+z_1+z_2}{2}\right)) \right) \left(1 + \frac{m_2}{z_2}\right) + \frac{m_1 m_2 P_2^{\frac{1}{2}(-z_1-z_2)}}{4\left(\frac{a_1}{a_2}\right)^{z_1}} \\
&\times \left(2 \ln \frac{a_1}{a_2} G_{3,0}^{2,3} \left(0, 0, \frac{1}{2}(1+z_1+z_2) \middle| P_2\right) - 2 G_{4,0}^{3,4} \left(0, 0, 0, \frac{1}{2}(1+z_1+z_2) \middle| P_2\right) \right) \\
&+ \Gamma\left(\frac{1}{2}(1+z_1+z_2)\right) \left(2 \ln \frac{a_1}{a_2} \ln P_2 + \ln^2 P_2 - 2 \ln \frac{a_1 P_2}{a_2} \psi^{(0)}\left(\frac{1+z_1+z_2}{2}\right) + \psi^{(0)}\left(\frac{1+z_1+z_2}{2}\right)^2 + \psi^{(1)}\left(\frac{1+z_1+z_2}{2}\right) \right) \Big]
\end{aligned} \tag{38}$$

where $P_1 = \frac{Ba_1^2 \gamma_0}{2}$ and $P_2 = \frac{Ba_2^2 \gamma_0}{2}$.

loss due to the fog.

IV. SIMULATION AND NUMERICAL ANALYSIS

In this section, we use numerical analysis and Monte Carlo (MC) simulation (averaged over 10^7 channel realizations) to demonstrate the performance of the relay-assisted OWC system under the combined effect of fog with pointing errors. We also provide simulation results using the exact

EW turbulence model and numerical results using the derived asymptotic analysis when the atmospheric turbulence is also considered. We consider three simulation scenarios: fog, pointing errors, and atmospheric turbulence (FPT), fog and pointing errors (FP), deterministic path loss with pointing errors, and atmospheric turbulence (PT). Although a direct link between the source and destination may not exist, we compare the performance of direct and relay-assisted transmissions at various link distances and pointing errors parameters. We also analyze the channel-assisted AF relaying by developing an integral-form expression for the PDF of the end-to-end SNR,

¹In many papers, it is wrongly written as A^2/Hz .

TABLE II
SIMULATION PARAMETERS

Transmitted power	P_t	0 to 40 dBm
Responsivity	R	0.5 A/W
AWGN variance	σ_w^2	10^{-14} A ² /GHz ¹
Link distance	d	500 m and 800 m
Shape parameter of fog	k	{2.32, 5.49, 6.00}
Scale parameter of fog	β	{13.12, 12.06, 23.00}
Aperture diameter	$D = 2a_r$	10 cm
Normalized beam-width	w_z/a_r	{15, 20, 25}
Normalized jitter	σ_s/a_r	{3, 5}
Refractive index	C_n^2	8×10^{-14}
Wavelength	λ	1550 nm
Turbulence parameters	$\{\alpha, \beta, \eta\}$	{3.02, 2.80, 0.84}

as presented in Appendix D. We validate our derived analytical expressions with numerical and simulation results. We use standard simulation parameters of the OWC system as given in Table II.

First, we demonstrate the mutual effects of different channel impairments on the OWC system by plotting the average SNR versus transmit power for a link distance of 800 m, as shown in Fig. 2. Comparing the PT (where deterministic path loss is considered) and FPT plots in Fig. 2a, we can find that the fixed visibility range based path-loss computation overestimate the average SNR by 10 dB with respect to the random path loss consideration. Further, the OWC system performs similarly for FP and FPT channels, as shown in Fig. 2a, since the effect of fading due to the atmospheric turbulence is negligible in the presence of fog. Moreover, it can also be seen that there is a small difference of around 2 dB in average SNR between our analysis for FP/FPT channels (which is based on integer-valued $k = 2$) with simulation results on real-valued $k = 2.32$. In Fig. 2b, we analyze the effect of pointing errors on the average SNR performance over light fog under the FPT channel and moderate fog under the FP channel considering the asymmetric placement of the relay. It can be seen from the figure that the average SNR performance decreases with an increase in normalized beam width and jitter. It should be noted that the effect of normalized beam width (w_z/a_r) on the average SNR performance is more as compared to the standard deviation of the normalized jitter (σ_s/a_r). It can be observed that there is a small benefit in the average SNR performance with the relaying system. However, it should be emphasized that the direct link may not exist, and relaying is necessary for the data transmission between the source and destination.

The ergodic rate performance in Fig. 3 shows a significant benefit of the relay-assisted system under FP and FPT channels. However, similar to the average SNR, the impact of atmospheric turbulence is found to be negligible on the ergodic rate in the presence of fog. The relay-assisted system gives more increment over moderate fog than the light fog as compared to the no-relay system. Moreover, the slopes at high transmit power show greater improvement with the relay-assisted transmission compared with the direct transmissions. Comparing Fig. 3a and Fig. 3b, it can be seen a greater

improvement in the ergodic rate performance using the asymmetric placement of the relay with a longer link length (i.e., 800 m) than a shorter one (i.e., 500 m). It can also be seen from Fig. 3b that the normalized beam width has a significant impact on the ergodic rate performance.

In Fig. 4a, we demonstrate the outage probability performance of the OWC system for three different fog conditions (i.e., light, moderate, and thick fog) at a normalized beam-width of ($w_z/a_r = 25$) and normalized standard deviation of the jitter ($\sigma_s/a_r = 3$). The figure shows that the relay-assisted transmission provides a significant gain in the outage performance comparing to the direct transmission for both symmetrical and asymmetrical relay positions. A better outage probability can be attributed to the lower path loss in the relayed system. Moreover, an increase in the fog density deteriorates the outage probability performance of the OWC system: transmission in moderate fog requires 15 dBm more transmit power to achieve the same outage probability (10^{-3} for the asymmetric condition at 25 dBm) in the light fog condition. Further, Fig. 4a shows that the symmetric relay position provides a higher gain in the outage performance comparing the asymmetric position of the relay between the source and destination. In Fig. 4b, we demonstrate the effect of pointing errors (i.e., normalized beam width and jitter) on the outage probability performance of an OWC system under FPT channel for light foggy condition and atmospheric turbulence ($C_n^2 = 8 \times 10^{-14}$ m^{-2/3}). We find a similar trend in the performance behavior of Fig. 4a, in addition to that, the outage probability decreases with an increase in normalized beam width since the fraction of collected power A_0 decreases.

Finally, in Fig. 5, we demonstrate the average BER performance of the OWC system with OOK modulation as a function of transmit power over the light foggy condition at different normalized beam-width of ($w_z/a_r = 15, 25$) and a normalized standard deviation of the jitter ($\sigma_s/a_r = 3$). Fig. 5a shows that the relay-assisted system provides a significant improvement in the average BER performance compared with the direct transmission, even with the same fading scenarios under the FP channel for a link distance of 500 m. The considered dual-hop relay assisted OWC system requires 15 dBm transmit power to achieve an average BER (10^{-3} which is considered reasonable for OWC applications) under the FP channel with the symmetric condition. Moreover, the symmetric relay position provides more gain than the asymmetric condition for the average BER compared with the average SNR and ergodic rate. Further, the impact of normalized beam width is more on the average BER, as shown in Fig. 5a. We also demonstrate the average BER performance under the FPT channel or a 800 m link system in Fig. 5b, which shows similar performance behavior, as observed for the FP channel.

In all the above plots (Fig. 2 to Fig. 5), we have also verified our derived expressions with the simulation and numerical results. It can be seen that the derived closed-form expressions of the outage probability, average SNR, ergodic rate, and average BER have an excellent match with the simulation results. However, there is a gap between simulation and analysis for the ergodic rate at a lower transmit power due to the use of inequality $\log_2(\gamma) \leq \log_2(1 + \gamma)$. Further, we have compared the AF relaying with the DF. It is expected that the DF relaying would perform better than the AF since $\gamma^{AF} = \frac{\gamma_1 \gamma_2}{\gamma_1 + \gamma_2 + 1} \leq \min(\gamma_1, \gamma_2) = \gamma^{DF}$, but the difference is marginal under the considered channel impairments. The

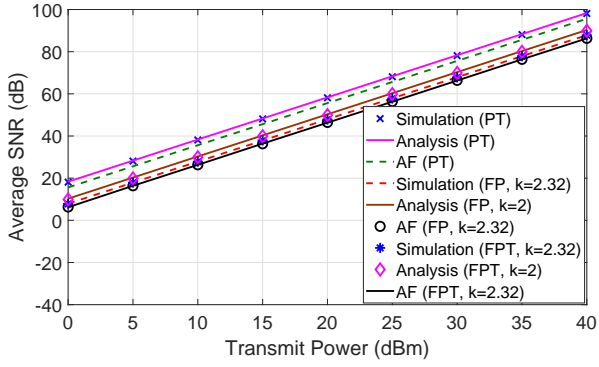
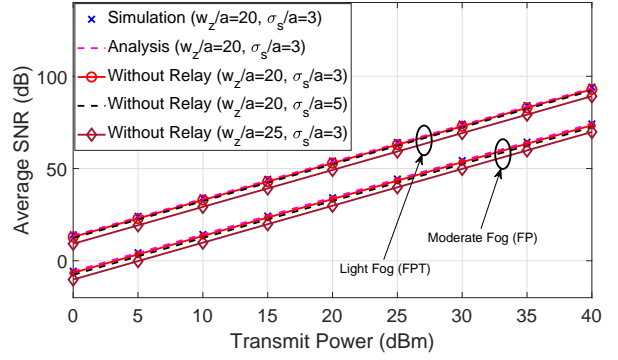
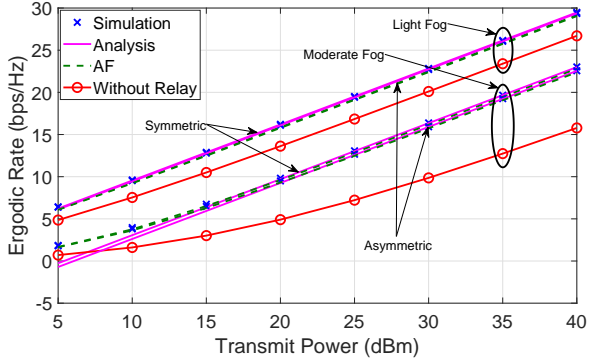
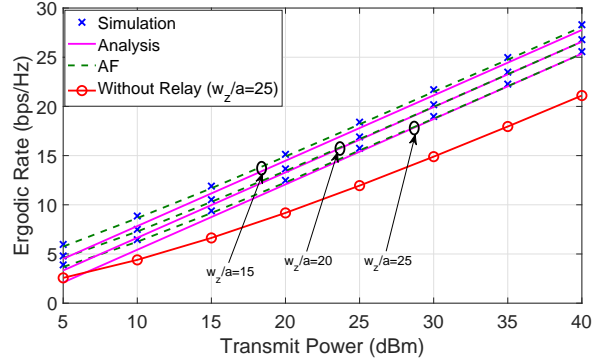
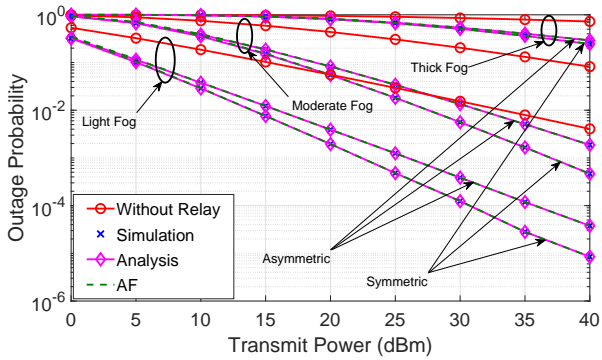
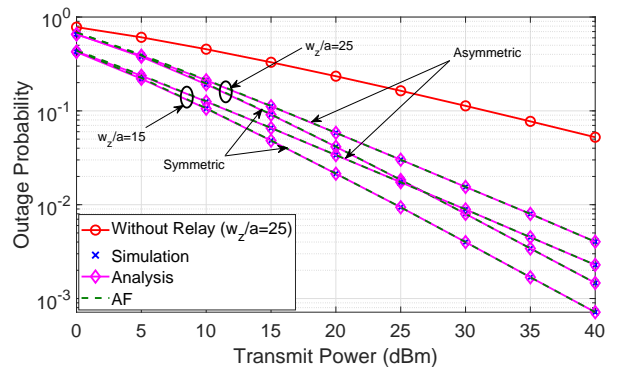
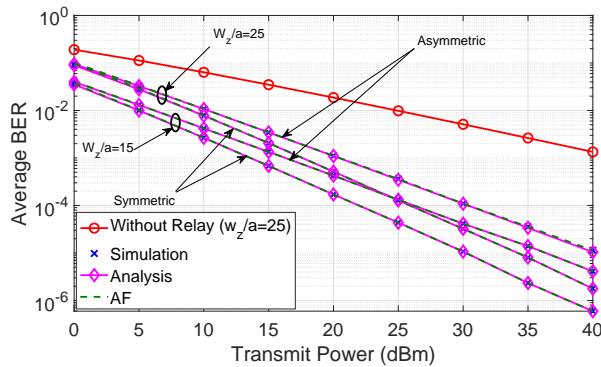
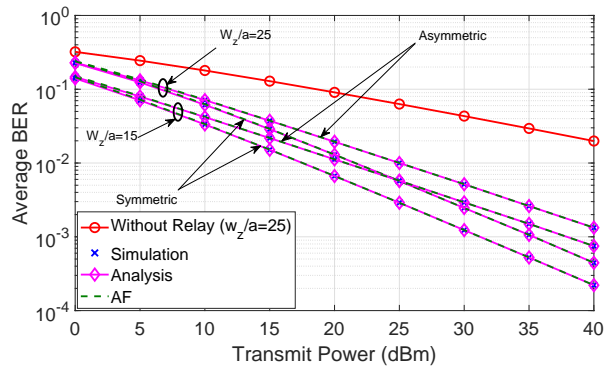
(a) Symmetrical: $d_1 = d_2 = 400$ with $w_z/a_r = 25$, $\sigma_s/a_r = 3$ m.(b) Asymmetrical: $d_1 = 300$ m, $d_2 = 500$ mFig. 2. Average SNR performance of relay-assisted OWC system for a transmission link $d = 800$ m.(a) FP channel for different fog conditions at $\sigma_s/a_r = 3$ and $w_z/a_r = 25$, asymmetrical: $d_1 = 200$ m, $d_2 = 300$ m, and symmetrical: $d_1 = d_2 = 250$ m.(b) FPT channel for different w_z/a_r at $\sigma_s/a_r = 3$ and asymmetrical relay position: $d_1 = 300$ m, $d_2 = 500$ m.

Fig. 3. Ergodic rate performance of relay-assisted OWC system.

(a) FP channel with $w_z/a_r = 25$, $\sigma_s/a_r = 3$, asymmetrical: $d_1 = 200$ m, $d_2 = 300$ m, and symmetrical: $d_1 = d_2 = 250$ m.(b) FPT channel with $\sigma_s/a_r = 3$ at different w_z/a_r , asymmetrical: $d_1 = 300$ m, $d_2 = 500$ m, and symmetrical: $d_1 = d_2 = 400$ m.Fig. 4. Outage performance of relay-assisted OWC system at a threshold SNR $\gamma_{th} = 6$ dB.



(a) FP channel with $\sigma_s/a_r = 3$ at different w_z/a_r , asymmetrical: $d_1 = 200$ m, $d_2 = 300$ m, and symmetrical: $d_1 = d_2 = 250$ m.



(b) FPT channel with $\sigma_s/a_r = 3$ at different w_z/a_r , asymmetrical: $d_1 = 300$ m, $d_2 = 500$ m, and symmetrical: $d_1 = d_2 = 400$ m.

Fig. 5. Average BER performance of relay-assisted OWC system.

performance channel-assisted AF and DF were also shown to be similar under certain scenarios over strong turbulence and pointing errors in [21].

V. CONCLUSIONS AND FUTURE WORK

In this paper, we investigated the performance of a DF relaying based OWC system under the combined effect of random fog, pointing errors, and atmospheric turbulence. We have shown that the dual-hop relaying is capable of mitigating fog, pointing errors, and turbulence-induced fading for high-speed OWC links. We analyzed the distribution functions of SNR and provided a detailed analysis for the outage probability, average SNR, ergodic rate, and average BER considering a generalized i.n.i.d fading model with asymmetrical distance for relaying between the source and destination. We have shown that there is a significant gap in the performance using the existing visibility range based path-loss computation as compared to the probabilistic modeling of fog. Further, the effect of fading due to atmospheric turbulence is shown to be negligible in the presence of fog. Moreover, the effect of normalized beam width on the OWC performance is more than the standard deviation of normalized jitter. It was also demonstrated that the relay-assisted system shows better performance than the direct-link transmissions as a benchmark, providing a more significant benefit in the denser fog, for longer link lengths, and when the relay is located symmetrically between the source and destination. Numerical analysis shows that the derived closed-form expressions excellently match with simulation results, and thus can be implemented for real-time tuning of the system parameters to optimize the OWC performance.

The proposed work can be augmented with several research directions. Although the asymptotic analysis using the combined effect of random fog, pointing errors, and atmospheric turbulence is close to the exact results, analyzing the exact PDF of the combined channel with different atmospheric turbulence models can be useful. We have also shown that there is a marginal difference between the performance of DF and AF relaying under the considered channel impairments. Thus, it would be interesting to investigate low complexity all-optical relaying schemes for OWC systems under the combined effect of fog, pointing errors, and atmospheric turbulence.

APPENDIX A (CLOSED-FORM EXPRESSIONS OF THEOREM 1)

For a better presentation, we present the closed-form expressions of average SNR and ergodic rate as derived in Theorem 1 in (45) and (46) respectively.

APPENDIX B (INTEGRALS OF THEOREM 1)

To solve the first and second integrals of (25), we substitute $\ln u = t$ and apply the definition of Gamma function and incomplete gamma function to get the following closed-form expressions:

$$\int_1^{\infty} u^{-n} (\ln(u))^p du = \frac{\Gamma[p+1]}{(n-1)^{p+1}} \quad (47)$$

$$\int_a^{\infty} u^{-n-3} (\ln(u))^p du = \frac{\Gamma[p+1, (2+n)\ln(a)]}{(2+n)^{p+1}} \quad (48)$$

Further, to solve the third integral of (25), we substitute $n \ln u = t$ and use the well-known identity $\int_0^{\infty} e^{-at} \Gamma(b, t) dt = a^{-1} \Gamma(b) (1 - (a+1)^{-b})$ [[55]–pp.657, eq. 6.451.2] to get the following:

$$\int_1^{\infty} u^{-n} \Gamma[k, n \ln u] du = \frac{(1 - n^k (2n-1)^{-k}) \Gamma[k]}{n-1} \quad (49)$$

Finally, we solve (26) by substituting $\ln u = t$ and $\ln a + t = v$ and apply the identity $\int_u^{\infty} x^{v-1} (x-u)^{\mu-1} e^{-bx} dx = b^{-\frac{\mu+v}{2}} u^{\frac{\mu+v-2}{2}} \Gamma(\mu) e^{-\frac{bu}{2}} W_{\frac{v-\mu}{2}, \frac{1-\mu-v}{2}}(bu)$ [[55]–pp.348, eq. 3.383.4] to get a closed-form expression in terms of Whittaker function, $W_{\lambda, \mu}(z)$ defined as:

$$W_{\lambda, \mu}(z) = \frac{\Gamma(-2\mu)}{\Gamma(\frac{1}{2} - \mu - \lambda)} M_{\lambda, \mu}(z) + \frac{\Gamma(2\mu)}{\Gamma(\frac{1}{2} + \mu - \lambda)} M_{\lambda, -\mu}(z) \quad (50)$$

where $M_{\lambda, \mu}(z)$ denotes the Whittaker M -function. Now, we express the Whittaker M -function in terms of confluent hypergeometric function [[55]–pp.1024, eq. 9.220.4] $M_{\lambda, \mu} = z^{\mu+\frac{1}{2}} e^{-z/2} \Phi(\mu - \lambda + \frac{1}{2}, 2\mu + 1 : z)$, $M_{\lambda, -\mu} =$

$$\begin{aligned}
\mathcal{F}_\gamma(a_1, a_2, \phi_1, \phi_2, z_1, z_2, k) = & 2 \left(\frac{C_1^{(1)} a_2^{2+\phi_1^2} \gamma_0}{(2+\phi_1^2)} - \frac{C_1^{(2)} a_1^{2+\phi_1^2} \gamma_0 (k-1)!}{(2+z_1)} \sum_{j=0}^{k-1} \frac{\left(\frac{m_1}{2+z_1}\right)^j \Gamma[1+j, (2+z_1) \ln\left(\frac{a_1}{a_2}\right)]}{j!} \right. \\
& + \frac{C_2^{(1)} a_2^{2+\phi_2^2} \gamma_0}{(2+\phi_2^2)} - \frac{C_2^{(2)} a_2^{2+\phi_2^2} \gamma_0 \Gamma[k]}{(2+\phi_2^2)} \left(1 - \left(\frac{2+z_2}{m_2}\right)^{-k} \right) - \frac{C_1^{(1)} D_2^{(1)} a_2^{2+\phi_1^2} \gamma_0}{(2+\phi_1^2+\phi_2^2)} + \\
& C_1^{(1)} D_2^{(2)} a_2^{2+\phi_1^2} \gamma_0 (k-1)! \sum_{i=0}^{k-1} \frac{m_2^i z_2^{-i-1} \Gamma(i+1) (\phi_1^2+z_2+2)^{-i-1} \left((\phi_1^2+z_2+2)^{i+1} - z_2^{i+1} \right)}{i! (\phi_1^2+2)} + \\
& \frac{C_1^{(2)} D_2^{(1)} a_1^{2+\Gamma_1^2} \left(\frac{a_1}{a_2}\right)^{\phi_2^2} \gamma_0 (k-1)!}{(2+z_1+\phi_2^2)} \sum_{j=0}^{k-1} \frac{\left(\frac{m_1}{2+z_1+\phi_2^2}\right)^j \Gamma[1+j, (2+z_1+\phi_2^2) \ln\left(\frac{a_1}{a_2}\right)]}{j!} - \\
& \frac{C_1^{(2)} D_2^{(2)} a_2^{2+\phi_1^2} \gamma_0}{\left(\frac{a_1}{a_2}\right)^{m_1} ((k-1)!)^{-2}} \sum_{i=0}^{k-1} \sum_{j=0}^{k-1} \sum_{t=0}^i \frac{m_2^i m_1^j z_1^{t-i-1}}{j! t! \Gamma[-j]} \left(\Gamma[-j] \Gamma[1+j+t] (2+z_1+z_2)^{-1-j-t} \right. \\
& \times {}_1F_1\left(-j; -j-t; (2+z_1+z_2) \ln\left(\frac{a_1}{a_2}\right)\right) + \Gamma[1+t] \Gamma[-1-j-t] \left(\ln\left(\frac{a_1}{a_2}\right)\right)^{1+j+t} \\
& \left. \times {}_1F_1\left(1+t; 2+j+t; (2+z_1+z_2) \ln\left(\frac{a_1}{a_2}\right)\right) - \frac{C_2^{(1)} D_1^{(1)} a_2^{2+\phi_2^2} \left(\frac{a_1}{a_2}\right)^{-\phi_1^2} \gamma_0}{(2+\phi_1^2+\phi_2^2)} + \right. \\
& \frac{C_2^{(1)} D_1^{(2)} a_2^{2+\phi_2^2} \gamma_0 (k-1)!}{(2+z_1+\phi_2^2)} \sum_{i=0}^{k-1} \frac{m_1^i z_1^{-i-1}}{i!} \left(\frac{\Gamma(1+i, z_1 \ln\left(\frac{a_1}{a_2}\right)) - \left(\frac{a_1}{a_2}\right)^{2+\phi_2^2} \left(\frac{z_1}{2+\phi_2^2+z_1}\right)^{i+1} \Gamma(1+i, (2+\phi_2^2+z_1) \ln\left(\frac{a_1}{a_2}\right))}{2+\phi_2^2} \right) \\
& \left. + \frac{C_2^{(2)} D_1^{(1)} a_2^{2+\phi_2^2} \left(\frac{a_1}{a_2}\right)^{-\phi_1^2} \gamma_0 \Gamma[k]}{(2+\phi_1^2+\phi_2^2)} \left(1 - \left(\frac{2+z_2+\phi_1^2}{m_2}\right)^{-k} \right) - \right. \\
& \frac{C_2^{(2)} D_1^{(2)} a_2^{2+\phi_1^2} \gamma_0}{\left(\frac{a_1}{a_2}\right)^{z_1} ((k-1)!)^{-2}} \sum_{i=0}^{k-1} \sum_{j=0}^{k-1} \sum_{t=0}^i \frac{m_1^i m_2^j z_1^{t-i-1}}{j! t! \Gamma[-t]} \left(\Gamma[-t] \Gamma[1+j+t] (2+z_1+z_2)^{-1-j-t} \right. \\
& \times {}_1F_1\left(-t; -j-t; (2+z_1+z_2) \ln\left(\frac{a_1}{a_2}\right)\right) + \\
& \left. \left. \Gamma[1+j] \Gamma[-1-j-t] \left(\ln\left(\frac{a_1}{a_2}\right)\right)^{1+j+t} {}_1F_1\left(1+j; 2+j+t; (2+z_1+z_2) \ln\left(\frac{a_1}{a_2}\right)\right) \right) \right) \quad (45)
\end{aligned}$$

$z^{-\mu+\frac{1}{2}} e^{-z/2} \Phi(-\mu-\lambda+\frac{1}{2}, -2\mu+1; z)$, where $\Phi(\alpha, \lambda; z) = {}_1F_1(\alpha; \lambda; z)$, we get the following:

$$\begin{aligned}
\int_1^\infty u^{-n} (\ln(au))^p (\ln(u))^t du = & \frac{\Gamma(1+p+t) {}_1F_1(-p; -p-t; (n-1) \ln(a))}{(n-1)^{1+p+t}} \\
& + \frac{\Gamma[-1-p-t] \Gamma[1+t] (\ln(a))^{1+p+t} {}_1F_1(1+t; 2+p+t; (n-1) \ln(a))}{\Gamma[-p]} \quad (51)
\end{aligned}$$

$$\begin{aligned}
& \text{get the following:} \\
& \int_a^\infty u^{-n-2} e^{-\frac{p}{u^2}} \ln(u) du = \frac{1}{4} p^{\frac{1}{2}(-n-1)} \\
& \left(\ln\left(\frac{1}{a^2}\right) \Gamma\left(\frac{1}{2}(n+1), \frac{p}{a^2}\right) + G_{2,3}^{3,0}\left(\frac{p}{a^2} \middle| 0, 0, \frac{n+1}{2}\right) \right. \\
& \left. + \Gamma\left(\frac{n+1}{2}\right) \left(\ln(p) - \psi^{(0)}\left(\frac{n+1}{2}\right)\right) \right) \quad (53)
\end{aligned}$$

Finally, to solve the third integral of (42), we apply the integration by parts twice, and then follow the same procedure used in deriving (53) to get:

$$\begin{aligned}
& \int_1^\infty u^{-n-2} e^{-\frac{p}{u^2}} \ln^2(u) du = \\
& \frac{1}{8} \left(-2G_{3,4}^{4,0}\left(p \middle| 0, \frac{1}{2}(-n-1), \frac{1-n}{2}, \frac{1-n}{2}, \frac{1-n}{2}\right) \right. \\
& \left. -2\left(\ln\left(\frac{1}{p}\right) + \ln(p)\right) G_{2,3}^{3,0}\left(p \middle| 0, \frac{1}{2}(-n-1), \frac{1-n}{2}, \frac{1-n}{2}\right) \right) \\
& + \left(\frac{1}{p}\right)^{\frac{n+1}{2}} \left(\Gamma\left(\frac{n+1}{2}\right) \left(2\psi^{(0)}\left(\frac{n+1}{2}\right) \ln\left(\frac{1}{p}\right) \right. \right. \\
& \left. \left. + \psi^{(0)}\left(\frac{n+1}{2}\right)^2 + \psi^{(1)}\left(\frac{n+1}{2}\right) + \ln^2\left(\frac{1}{p}\right) \right) - \right. \\
& \left. \left(\ln\left(\frac{1}{p}\right) + \ln(p)\right)^2 \Gamma\left(\frac{n+1}{2}, p\right) \right) \quad (54)
\end{aligned}$$

APPENDIX C (INTEGRALS OF THEOREM 2)

To solve the first integral of (42), we use $\int_1^\infty f(t) dt = \int_0^\infty f(t) dt - \int_0^a f(t) dt$, and apply the definition of Gamma function and incomplete Gamma function. After a few simplifications, we get the following closed-form expression:

$$\int_1^\infty u^{-n-2} e^{-\frac{p}{u^2}} du = \frac{1}{2} \left(\frac{1}{p}\right)^{\frac{n+1}{2}} \left(\Gamma\left(\frac{n+1}{2}\right) - \Gamma\left(\frac{n+1}{2}, p\right) \right) \quad (52)$$

For the second integral of (42), we again use $\int_1^\infty f(t) dt = \int_0^\infty f(t) dt - \int_0^a f(t) dt$, and apply the integration by parts on both the terms. Using the identity $\int_0^\infty t^{v-1} e^{-ut} \ln(t) dt = u^{-v} \Gamma(v) (\psi^{(0)}(v) - \ln(u))$ [[55]–pp.573, eq. 4.352.1], and the identity of Meijer's G function [[61], eq. (07.34.21.0084.01)], we

$$\begin{aligned}
\mathcal{F}_\eta(a_1, a_2, \phi_1, \phi_2, z_1, z_2, k) = & \log_2\left(\frac{e}{2\pi}\right) + 2.8854 \left[\frac{C_1^{(1)} a_2^{\phi_1^2} (-2 + \phi_1^2 \ln(a_2^2 \gamma_0))}{\phi_1^2} + \frac{C_2^{(1)} a_2^{\phi_2^2} (-2 + \phi_2^2 \ln(a_2^2 \gamma_0))}{\phi_2^2} - \right. \\
& C_1^{(2)} a_1^{\phi_1^2} (k-1)! \sum_{i=0}^{k-1} \frac{m_1^i \left(z_1 \Gamma\left(1+i, z_1 \ln\left(\frac{a_1}{a_2}\right)\right) \ln(a_1^2 \gamma_0) - 2\Gamma\left(2+i, z_1 \ln\left(\frac{a_1}{a_2}\right)\right) \right)}{i! z_1^{2+i}} - \\
& C_2^{(2)} a_2^{\phi_2^2} (k-1)! \sum_{i=0}^{k-1} \frac{m_2^i (-2(1+i) + z_2 \ln(a_2^2 \gamma_0))}{z_2^{2+i}} - \frac{C_1^{(1)} D_2^{(1)} a_2^{\phi_1^2} (-2 + (\phi_1^2 + \phi_2^2) \ln(a_2^2 \gamma_0))}{(\phi_1^2 + \phi_2^2)^2} + \\
& C_1^{(1)} D_2^{(2)} a_2^{\phi_1^2} (k-1)! \sum_{i=0}^{k-1} \sum_{j=0}^i \frac{m_2^i z_2^{j-i-1} (-2(1+j) + (\phi_1^2 + z_2) \ln(a_2^2 \gamma_0))}{(\phi_1^2 + z_2)^{2+j}} + \\
& C_1^{(2)} D_2^{(1)} a_1^{\phi_1^2} \left(\frac{a_1}{a_2}\right)^{\phi_2^2} (k-1)! \sum_{i=0}^{k-1} \frac{m_1^i \left(-2\Gamma\left(2+i, (\phi_2^2 + z_1) \ln\left(\frac{a_1}{a_2}\right)\right) + (\phi_2^2 + z_1) \Gamma\left(1+i, (\phi_2^2 + z_1) \ln\left(\frac{a_1}{a_2}\right)\right) \ln(a_1^2 \gamma_0) \right)}{i! (\phi_2^2 + z_1)^{2+i}} \\
& - C_1^{(2)} D_2^{(2)} a_2^{\phi_1^2} \left(\frac{a_1}{a_2}\right)^{-m_1} ((k-1)!)^2 \sum_{k-1}^{i=0} \sum_{j=0}^{k-1} \sum_{t=0}^i \frac{m_1^i m_2^j z_2^{t-i-1}}{j! t! \Gamma[-j]} \\
& \times \left((z_1 + z_2)^{-1-j-t} \left(\Gamma[-j] \Gamma[1+j+t] {}_1F_1\left(-j; -j-t; (z_1 + z_2) \ln\left(\frac{a_1}{a_2}\right)\right) + \right. \right. \\
& \left. \Gamma[1+t] \Gamma[-1-j-t] {}_1F_1\left(1+t; 2+j+t; (z_1 + z_2) \ln\left(\frac{a_1}{a_2}\right)\right) \left((z_1 + z_2) \ln\left(\frac{a_1}{a_2}\right) \right)^{1+j+t} \right) \\
& \times (2 \ln(a_2) + \ln(\gamma_0)) - 2\Gamma[2+t] \Gamma[-2-j-t] {}_1F_1\left(2+t; 3+j+t; (z_1 + z_2) \ln\left(\frac{a_1}{a_2}\right)\right) \ln^{2+j+t}\left(\frac{a_1}{a_2}\right) \\
& \left. - 2(z_1 + z_2)^{-2-j-t} \Gamma[-j] \Gamma[2+j+t] {}_1F_1\left(-j; -1-j-t; (z_1 + z_2) \ln\left(\frac{a_1}{a_2}\right)\right) \right) \\
& - \frac{C_2^{(1)} D_1^{(1)} a_2^{\phi_2^2} \left(\frac{a_2}{a_1}\right)^{\phi_1^2} (-2 + (\phi_1^2 + \phi_2^2) \ln(a_2^2 \gamma_0))}{(\phi_1^2 + \phi_2^2)^2} + C_2^{(1)} D_1^{(2)} a_1^{\phi_2^2} (k-1)! \\
& \times \sum_{i=0}^{k-1} \sum_{j=0}^i \frac{m_1^i z_1^{j-i-1} \left(-2\Gamma\left(2+j, (\phi_2^2 + z_1) \ln\left(\frac{a_2}{a_1}\right)\right) + (\phi_2^2 + z_1) \Gamma\left(1+j, (\phi_2^2 + z_1) \ln\left(\frac{a_2}{a_1}\right)\right) \ln(a_2^2 \gamma_0) \right)}{j! (\phi_2^2 + z_1)^{2+j}} + \\
& C_2^{(2)} D_1^{(1)} a_2^{\phi_2^2} \left(\frac{a_1}{a_2}\right)^{-\phi_1^2} (k-1)! \sum_{i=0}^{k-1} \frac{m_2^i (-2(1+i) + (\phi_1^2 + z_2) \ln(a_2^2 \gamma_0))}{(\phi_1^2 + z_2)^{2+i}} - \\
& C_2^{(2)} D_1^{(2)} a_2^{\phi_2^2} \left(\frac{a_1}{a_2}\right)^{-z_1} ((k-1)!)^2 \sum_{k-1}^{i=0} \sum_{j=0}^{k-1} \sum_{t=0}^i \frac{m_1^i m_2^j z_1^{t-i-1}}{j! t! \Gamma[-t]} \\
& \times \left((z_1 + z_2)^{-1-j-t} \left(\Gamma[-t] \Gamma[1+j+t] {}_1F_1\left(-t; -j-t; (z_1 + z_2) \ln\left(\frac{a_1}{a_2}\right)\right) + \right. \right. \\
& \left. \Gamma[1+j] \Gamma[-1-j-t] {}_1F_1\left(1+j; 2+j+t; (z_1 + z_2) \ln\left(\frac{a_1}{a_2}\right)\right) \left((z_1 + z_2) \ln\left(\frac{a_1}{a_2}\right) \right)^{1+j+t} \right) \times \\
& (2 \ln(a_2) + \ln(\gamma_0)) - 2\Gamma[2+j] \Gamma[-2-j-t] {}_1F_1\left(2+j; 3+j+t; (z_1 + z_2) \ln\left(\frac{a_1}{a_2}\right)\right) \ln^{2+j+t}\left(\frac{a_1}{a_2}\right) \\
& \left. - 2(z_1 + z_2)^{-2-j-t} \Gamma[-t] \Gamma[2+j+t] {}_1F_1\left(-t; -1-j-t; (z_1 + z_2) \ln\left(\frac{a_1}{a_2}\right)\right) \right) \left. \right] \quad (46)
\end{aligned}$$

APPENDIX D
(PDF OF AMPLIFY-AND-FORWARD RELAYING)

To derive a tractable analytical expression of the PDF of end-to-end SNR for the AF relaying, we ignore the 1 (since the PDF value is small for $\gamma < 1$) in the numerator of (8) to get:

$$\gamma < \frac{\gamma_1 \gamma_2}{\gamma_1 + \gamma_2} \quad (55)$$

Denoting the PDF of γ_1 and γ_2 as $f_1(\gamma)$ and $f_2(\gamma_2)$, respectively, we evaluate the PDFs of $1/\gamma_1$ and $1/\gamma_2$ using the inverse distribution, and employ the PDF of their sum [[62] eq.5.55] to get the resulting PDF of γ_{e2e} as

$$f(\gamma) = \gamma \int_{t_{min}}^{t_{max}} f_1\left(\frac{\gamma}{t}\right) f_2\left(\frac{\gamma}{1-t}\right) \frac{dt}{t^2(1-t)^2} \quad (56)$$

Considering the logarithmic term in (9) positive and applying this

constraint to $f_1\left(\frac{\gamma}{t}\right)$ and $f_2\left(\frac{\gamma}{1-t}\right)$, we get the limits of integration in (56) as $\ln\left(\frac{a^2 \gamma_0 t}{\gamma}\right) > 0 \implies t > \frac{a^2 \gamma_0}{\gamma} = t_{min}$, and $\ln\left(\frac{a^2 \gamma_0 (1-t)}{\gamma}\right) > 0 \implies t < 1 - \frac{a^2 \gamma_0}{\gamma} = t_{max}$. Note that using these limits, we can get the exact PDF in (56).

REFERENCES

- [1] M. A. Khalighi and M. Uysal, "Survey on free space optical communication: A communication theory perspective," *IEEE Commun. Surveys Tuts.*, vol. 16, no. 4, pp. 2231–2258, Fourthquarter 2014.
- [2] S. Bloom *et al.*, "Understanding the performance of free-space optics [Invited]," *J. Opt. Netw.*, vol. 2, no. 6, pp. 178–200, Jun 2003.
- [3] D. Kedar and S. Arnon, "Urban optical wireless communication networks: the main challenges and possible solutions," *IEEE Commun. Mag.*, vol. 42, no. 5, pp. S2–S7, May 2004.
- [4] A. A. Farid and S. Hranilovic, "Outage capacity optimization for free-space optical links with pointing errors," *J. Lightw. Technol.*, vol. 25, no. 7, pp. 1702–1710, July 2007.

- [5] A. Vavoulas *et al.*, "Weather effects on FSO network connectivity," *IEEE/OSA J. Opt. Commun. Netw.*, vol. 4, no. 10, pp. 734–740, Oct 2012.
- [6] P. W. Kruse *et al.*, *Elements of Infrared Technology: Generation, Transmission and Detection*. New York: Wiley, 1962, vol. 1.
- [7] I. I. Kim *et al.*, "Comparison of laser beam propagation at 785 nm and 1550 nm in fog and haze for optical wireless communications," *Proc. SPIE*, vol. 4214, pp. 26–37, Nov. 2001.
- [8] D. Bushuev and S. Arnon, "Analysis of the performance of a wireless optical multi-input to multi-output communication system," *J. Opt. Soc. Am. A*, vol. 23, no. 7, pp. 1722–1730, Jul 2006.
- [9] M. Safari and M. Uysal, "Relay-assisted free-space optical communication," *IEEE Trans. Wireless Commun.*, vol. 7, no. 12, pp. 5441–5449, 2008.
- [10] S. M. Aghajanzadeh and M. Uysal, "Multi-hop coherent free-space optical communications over atmospheric turbulence channels," *IEEE Trans. Commun.*, vol. 59, no. 6, pp. 1657–1663, 2011.
- [11] E. Zedini and M. Alouini, "Multihop relaying over IM/DD FSO systems with pointing errors," *J. Lightw. Technol.*, vol. 33, no. 23, pp. 5007–5015, Dec 2015.
- [12] N. D. Chatzidiamantis *et al.*, "Relay selection protocols for relay-assisted free-space optical systems," *IEEE/OSA J. Opt. Commun. Netw.*, vol. 5, no. 1, pp. 92–103, 2013.
- [13] S. Molla Aghajanzadeh and M. Uysal, "Performance analysis of parallel relaying in free-space optical systems," *IEEE Trans. Commun.*, vol. 63, no. 11, pp. 4314–4326, 2015.
- [14] M. A. Kashani *et al.*, "Optimal relay placement and diversity analysis of relay-assisted free-space optical communication systems," *IEEE/OSA J. Opt. Commun. Netw.*, vol. 5, no. 1, pp. 37–47, Jan 2013.
- [15] C. Abou-Rjeily and Z. Noun, "Impact of inter-relay co-operation on the performance of FSO systems with any number of relays," *IEEE Trans. Wireless Commun.*, vol. 15, no. 6, pp. 3796–3809, June 2016.
- [16] M. Karimi and M. Nasiri-Kenari, "Free space optical communications via optical amplify-and-forward relaying," *J. Lightw. Technol.*, vol. 29, no. 2, pp. 242–248, 2011.
- [17] Shabnam Kazemlou *et al.*, "All-optical multihop free-space optical communication systems," *J. Lightwave Technol.*, vol. 29, no. 18, pp. 2663–2669, Sep 2011.
- [18] E. Bayaki, D. S. Michalopoulos, and R. Schober, "EDFA-based all-optical relaying in free-space optical systems," *IEEE Trans. Commun.*, vol. 60, no. 12, pp. 3797–3807, 2012.
- [19] M. A. Kashani *et al.*, "All-optical amplify-and-forward relaying system for atmospheric channels," *IEEE Commun. Lett.*, vol. 16, no. 10, pp. 1684–1687, 2012.
- [20] P. V. Trinh *et al.*, "All-optical relaying FSO systems using EDFA combined with optical hard-limiter over atmospheric turbulence channels," *J. Lightw. Technol.*, vol. 33, no. 19, pp. 4132–4144, 2015.
- [21] L. Yang *et al.*, "Performance analysis of relay-assisted all-optical FSO networks over strong atmospheric turbulence channels with pointing errors," *J. Lightw. Technol.*, vol. 32, no. 23, pp. 4613–4620, Dec 2014.
- [22] E. Zedini *et al.*, "Dual hop FSO transmission systems over Gamma Gamma turbulence with pointing errors," *IEEE Trans. Wireless Commun.*, vol. 16, no. 2, pp. 784–796, Feb 2017.
- [23] M. T. Dabiri and S. M. S. Sadough, "Performance analysis of all-optical amplify and forward relaying over log-normal FSO channels," *IEEE/OSA J. Opt. Commun. Netw.*, vol. 10, no. 2, pp. 79–89, 2018.
- [24] X. Huang *et al.*, "Performance comparison of all-optical amplify-and-forward relaying FSO communication systems with OOK and DPSK modulations," *IEEE Photon. J.*, vol. 10, no. 4, pp. 1–11, 2018.
- [25] M. S. Khan *et al.*, "Selecting a distribution function for optical attenuation in dense continental fog conditions," in *2009 Int. Conf. on Emerg. Technol.*, 2009, pp. 142–147.
- [26] M. A. Esmail *et al.*, "Outdoor FSO communications under fog: Attenuation modeling and performance evaluation," *IEEE Photon. J.*, vol. 8, no. 4, pp. 1–22, Aug 2016.
- [27] —, "On the performance of optical wireless links over random foggy channels," *IEEE Access*, vol. 5, pp. 2894–2903, 2017.
- [28] Z. Rahman *et al.*, "Performance of opportunistic receiver beam selection in multiaperture OWC systems over foggy channels," *IEEE Syst. J.*, vol. 14, no. 3, pp. 4036–4046, 2020.
- [29] G. Schimmel *et al.*, "Free space laser telecommunication through fog," *Optica*, vol. 5, no. 10, pp. 1338–1341, Oct 2018.
- [30] M. A. Esmail *et al.*, "Outage probability analysis of FSO links over foggy channel," *IEEE Photon. J.*, vol. 9, no. 2, pp. 1–12, 2017.
- [31] Z. Rahman *et al.*, "Performance of opportunistic beam selection for OWC system under foggy channel with pointing error," *IEEE Commun. Lett.*, vol. 24, no. 9, pp. 2029–2033, Sep. 2020.
- [32] D. Kedar and S. Arnon, "Optical wireless communication through fog in the presence of pointing errors," *Appl. Opt.*, vol. 42, no. 24, pp. 4946–4954, Aug. 2003.
- [33] M. Al Naboulsi, "Fog attenuation prediction for optical and infrared waves," *Opt. Eng.*, vol. 43, no. 2, pp. 319–329, 2004.
- [34] M. Saleem Awan *et al.*, "Attenuation analysis for optical wireless link measurements under moderate continental fog conditions at Milan and Graz," in *IEEE 68th Veh. Technol. Conf. (VTC) 2008*, 2008, pp. 1–5.
- [35] M. A. Esmail *et al.*, "Analysis of fog effects on terrestrial free space optical communication links," in *2016 IEEE Int. Conf. on Commun. Wkshp. (ICC)*, May 2016, pp. 151–156.
- [36] P. Wilke Berenguer *et al.*, "Optical wireless MIMO experiments in an industrial environment," *IEEE J. Sel. Areas Commun.*, vol. 36, no. 1, pp. 185–193, Jan 2018.
- [37] X. Zhu and J. M. Kahn, "Free-space optical communication through atmospheric turbulence channels," *IEEE Trans. Commun.*, vol. 50, no. 8, pp. 1293–1300, 2002.
- [38] L. C. Andrews and R. L. Phillips, *Laser Beam Propagation Through Random Media*, vol. 1. Bellingham: SPIE, 2005, vol. 1.
- [39] A. Jurado-Navas *et al.*, "A unifying statistical model for atmospheric optical scintillation," *Numerical Simulations of Physical and Engineering Processes*, Sep 2011.
- [40] K. P. Peppas *et al.*, "The fisher–snedecor \mathcal{F} -distribution model for turbulence-induced fading in free-space optical systems," *J. Lightw. Technol.*, vol. 38, no. 6, pp. 1286–1295, 2020.
- [41] R. Barrios and F. Dios, "Exponentiated Weibull distribution family under aperture averaging for Gaussian beam waves," *Optics Express*, vol. 20, no. 12, pp. 13055–13064, Jun 2012.
- [42] K. Wardhan and S. Zafaruddin, "Simplified performance analysis of OWC system over atmospheric turbulence with pointing error," to appear in the *92nd IEEE Veh. Technol. Conf. (VTC) 2020-Fall*, 2020.
- [43] A. Nosratinia *et al.*, "Cooperative communication in wireless networks," *IEEE Commun. Mag.*, vol. 42, no. 10, pp. 74–80, 2004.
- [44] Q. Li *et al.*, "Cooperative communications for wireless networks: techniques and applications in LTE-advanced systems," *IEEE Wireless Commun.*, vol. 19, no. 2, pp. 22–29, 2012.
- [45] E. Lee *et al.*, "Performance analysis of the asymmetric dual-hop relay transmission with mixed RF/FSO links," *IEEE Photon. Technol. Lett.*, vol. 23, no. 21, pp. 1642–1644, 2011.
- [46] I. S. Ansari *et al.*, "Impact of pointing errors on the performance of mixed RF/FSO dual-hop transmission systems," *IEEE Wireless Commun. Lett.*, vol. 2, no. 3, pp. 351–354, 2013.
- [47] H. Samimi and M. Uysal, "End-to-end performance of mixed RF/FSO transmission systems," *IEEE/OSA J. Opt. Commun. Netw.*, vol. 5, no. 11, pp. 1139–1144, 2013.
- [48] S. Anees and M. R. Bhatnagar, "Performance of an amplify-and-forward dual hop asymmetric RF-FSO communication system," *IEEE/OSA J. Opt. Commun. Netw.*, vol. 7, no. 2, pp. 124–135, February 2015.
- [49] L. Kong *et al.*, "Performance of a free-space-optical relay-assisted hybrid RF/FSO system in generalized M -distributed channels," *IEEE Photon. J.*, vol. 7, no. 5, pp. 1–19, Oct 2015.
- [50] E. Zedini *et al.*, "On the performance analysis of dual-hop mixed FSO/RF systems," *IEEE Trans. Wireless Commun.*, vol. 15, no. 5, pp. 3679–3689, May 2016.
- [51] B. Bag *et al.*, "Performance analysis of hybrid FSO systems using FSO/RF-FSO link adaptation," *IEEE Photon. J.*, vol. 10, no. 3, pp. 1–17, 2018.
- [52] Y. Zhang *et al.*, "On the performance of dual-hop systems over mixed FSO/mmWave fading channels," *IEEE Open J. Commun. Soc.*, vol. 1, pp. 477–489, 2020.
- [53] R. Boluda-Ruiz *et al.*, "Outage performance of exponentiated Weibull FSO links under generalized pointing errors," *J. Lightwave Technol.*, vol. 35, no. 9, pp. 1605–1613, May 2017.
- [54] A. Papoulis and U. Pillai, *Probability, random variables and stochastic processes*, 4th ed. McGraw-Hill, Nov. 2001.
- [55] D. Zwillinger, *Table of integrals, series, and products*. Elsevier, 2014.
- [56] X. Song, F. Yang, and J. Cheng, "Subcarrier intensity modulated optical wireless communications in atmospheric turbulence with pointing errors," *IEEE/OSA Journal of Optical Communications and Networking*, vol. 5, no. 4, pp. 349–358, 2013.
- [57] F. Yang, J. Cheng, and T. A. Tsiftsis, "Free-space optical communication with nonzero boresight pointing errors," *IEEE Transactions on Communications*, vol. 62, no. 2, pp. 713–725, 2014.
- [58] Proakis, *Digital Communications 5th Edition*. McGraw Hill, 2007.
- [59] A. A. Boulgeorgos and A. Alexiou, "Error analysis of mixed THz-RF wireless systems," *IEEE Commun. Lett.*, vol. 24, no. 2, pp. 277–281, 2020.
- [60] M. A. Esmail *et al.*, "Experimental demonstration of outdoor 2.2 Tbps super-channel FSO transmission system," in *2016 IEEE Int. Conf. on Commun. Wkshp. (ICC)*, 2016, pp. 169–174.
- [61] Wolfram. (2001) The Wolfram functions site. Internet. [Online]. Available: <http://functions.wolfram.com>
- [62] T.T. Soong, *Fundamentals of Probability and Statistics for Engineers*. Wiley, 2004.